

## Article

# Simulation of Organic Liquid Products Deoxygenation by Multistage Countercurrent Absorber/Stripping Using CO<sub>2</sub> as Solvent with Aspen-HYSYS: Thermodynamic Data Basis and EOS Modeling

Elinéia Castro Costa <sup>1</sup>, Welisson de Araújo Silva <sup>1</sup>, Eduardo Gama Ortiz Menezes <sup>2</sup>, Marcilene Paiva da Silva <sup>2</sup>, Vânia Maria Borges Cunha <sup>2</sup>, Andréia de Andrade Mâncio <sup>1</sup>, Marcelo Costa Santos <sup>1</sup>, Sílvio Alex Pereira da Mota <sup>1</sup>, Marilena Emmi Araújo <sup>2</sup> and Nélio Teixeira Machado <sup>1,2,3,\*</sup>



**Citation:** Costa, E.C.; de Araújo Silva, W.; Menezes, E.G.O.; da Silva, M.P.; Cunha, V.M.B.; de Andrade Mâncio, A.; Santos, M.C.; da Mota, S.A.P.; Araújo, M.E.; Machado, N.T. Simulation of Organic Liquid Products Deoxygenation by Multistage Countercurrent Absorber/Stripping Using CO<sub>2</sub> as Solvent with Aspen-HYSYS: Thermodynamic Data Basis and EOS Modeling. *Molecules* **2021**, *26*, 4382. <https://doi.org/10.3390/molecules26144382>

Academic Editors: Stefano Cardea, Antonio Tabernero de Paz and Silvio A. B. Vieira de Melo

Received: 1 May 2021  
Accepted: 30 June 2021  
Published: 20 July 2021

**Publisher's Note:** MDPI stays neutral with regard to jurisdictional claims in published maps and institutional affiliations.



**Copyright:** © 2021 by the authors. Licensee MDPI, Basel, Switzerland. This article is an open access article distributed under the terms and conditions of the Creative Commons Attribution (CC BY) license (<https://creativecommons.org/licenses/by/4.0/>).

- <sup>1</sup> Graduate Program of Natural Resources Engineering of Amazon, Rua Corrêa N° 1, Campus Profissional-UFPA, Belém 66075-110, Pará, Brazil; elineia.costa.ec@gmail.com (E.C.C.); wasilva89@hotmail.com (W.d.A.S.); dedeiaam@yahoo.com.br (A.d.A.M.); marceloenqui@bol.com.br (M.C.S.); silviomota@unifesspa.edu.br (S.A.P.d.M.)
- <sup>2</sup> Graduate Program of Chemical Engineering, Rua Corrêa N° 1, Campus Profissional-UFPA, Belém 66075-110, Pará, Brazil; ortizegom@hotmail.com (E.G.O.M.); arci\_paiva@hotmail.com (M.P.d.S.); vaniacunha21@hotmail.com (V.M.B.C.); mearaajujo@gmail.com (M.E.A.)
- <sup>3</sup> Faculty of Sanitary and Environmental Engineering, Rua Corrêa N° 1, Campus Profissional-UFPA, Belém 66075-123, Pará, Brazil
- \* Correspondence: proderna@ufpa.br or ppgeq@ufpa.br; Tel.: +55-91-984620325

**Abstract:** In this work, the thermodynamic data basis and equation of state (EOS) modeling necessary to simulate the fractionation of organic liquid products (OLP), a liquid reaction product obtained by thermal catalytic cracking of palm oil at 450 °C, 1.0 atmosphere, with 10% (wt.) Na<sub>2</sub>CO<sub>3</sub> as catalyst, in multistage countercurrent absorber/stripping columns using supercritical carbon dioxide (SC-CO<sub>2</sub>) as solvent, with Aspen-HYSYS was systematically investigated. The chemical composition of OLP was used to predict the density ( $\rho$ ), boiling temperature ( $T_b$ ), critical temperature ( $T_c$ ), critical pressure ( $P_c$ ), critical volume ( $V_c$ ), and acentric factor ( $\omega$ ) of all the compounds present in OLP by applying the group contribution methods of Marrero-Gani, Han-Peng, Marrero-Pardillo, Constantinou-Gani, Joback and Reid, and Vetere. The RK-Aspen EOS used as thermodynamic fluid package, applied to correlate the experimental phase equilibrium data of binary systems OLP-<sub>i</sub>/CO<sub>2</sub> available in the literature. The group contribution methods selected based on the lowest relative average deviation by computing  $T_b$ ,  $T_c$ ,  $P_c$ ,  $V_c$ , and  $\omega$ . For *n*-alkanes, the method of Marrero-Gani selected for the prediction of  $T_c$ ,  $P_c$  and  $V_c$ , and that of Han-Peng for  $\omega$ . For alkenes, the method of Marrero-Gani selected for the prediction of  $T_b$  and  $T_c$ , Marrero-Pardillo for  $P_c$  and  $V_c$ , and Han-Peng for  $\omega$ . For unsubstituted cyclic hydrocarbons, the method of Constantinou-Gani selected for the prediction of  $T_b$ , Marrero-Gani for  $T_c$ , Joback for  $P_c$  and  $V_c$ , and the undirected method of Vetere for  $\omega$ . For substituted cyclic hydrocarbons, the method of Constantinou-Gani selected for the prediction of  $T_b$  and  $P_c$ , Marrero-Gani for  $T_c$  and  $V_c$ , and the undirected method of Vetere for  $\omega$ . For aromatic hydrocarbon, the method of Joback selected for the prediction of  $T_b$ , Constantinou-Gani for  $T_c$  and  $V_c$ , Marrero-Gani for  $P_c$ , and the undirected method of Vetere for  $\omega$ . The regressions show that RK-Aspen EOS was able to describe the experimental phase equilibrium data for all the binary pairs undecane-CO<sub>2</sub>, tetradecane-CO<sub>2</sub>, pentadecane-CO<sub>2</sub>, hexadecane-CO<sub>2</sub>, octadecane-CO<sub>2</sub>, palmitic acid-CO<sub>2</sub>, and oleic acid-CO<sub>2</sub>, showing average absolute deviation for the liquid phase ( $AAD_x$ ) between 0.8% and 1.25% and average absolute deviation for the gaseous phase ( $AAD_y$ ) between 0.01% to 0.66%.

**Keywords:** OLP; thermodynamic data basis; EOS Modeling; process simulation; Aspen-HYSYS

## 1. Introduction

The OLP obtained by thermal catalytic cracking of lipid-base materials, including vegetable oils [1–17], residual oils [18–25], animal fats [26–28], residual animal fat [27], mixtures of carboxylic acids [28–33], soaps of carboxylic acids [34,35], and scum, grease & fats [36–38], may be used as liquid fuels [1,2,4–8,10,11,13–20,22,26,35–41], if proper upgrading processes (distillation, adsorption, and liquid-liquid extraction) are applied to remove the oxygenates [6,7,10,16–19,35–41].

In order to be used as a liquid fuel, the upgraded and/or de-acidified OLP, must also match the most important physicochemical (acid value, flash point, carbon residue, cloud point, water in sediments, copper corrosiveness), physical (density), and transport properties (kinematic viscosity) to fossil-fuel specifications [10,16–19,35–41].

The OLP composed by alkanes, alkenes, ring-containing alkanes, ring-containing alkenes, cycloalkanes, cycloalkenes, and aromatics [4,8,10,16–19,26,28,29,34–38], as well as oxygenates including carboxylic acids, aldehydes, ketones, fatty alcohols, and esters [4,6–8,10,16,17,26,28,34–41].

A process with great potential to remove and/or recover oxygenates from OLP (De-acidification of OLP) is multistage gas extraction, using SC-CO<sub>2</sub> as solvent, based on similar studies reported in the literature [42,43]. However, knowledge of phase equilibrium for the complex system OLP/CO<sub>2</sub> is necessary.

The knowledge of phase equilibrium data is of fundamental importance for the design of equilibrium-stage separation processes (e.g., multistage gas extraction, absorption, liquid-liquid extraction, distillation), as it provides the thermodynamic basis for the separation process analysis [44].

High pressure phase equilibrium data yields information concerning the solubility of the coexisting gas-liquid phases, solvent capacity, compositions of the coexisting phases, distribution coefficients, and selectivity [44]. Those measurements are time consuming, needs special infrastructure (equilibrium cells, sampling units, and compressors), sophisticated chemical analysis (GC-MS, HPLC, etc.), and qualified human resources, thus posing not only a complex experimental task, but also high investment and operational costs [44,45].

In this context, the construction of a thermodynamic data basis is necessary for the modeling of complex/multi-component mixtures/CO<sub>2</sub> using EOS. Process thermodynamic modeling of complex mixtures/CO<sub>2</sub> using EOS, is a powerful tool to provide preliminary information of high-pressure phase equilibrium of complex multi-component systems/CO<sub>2</sub>, for guiding experimental high-pressure phase equilibrium measurements, as well as to reduce the number of necessary experiments, but not to replace experimental data [45].

Modern design of equilibrium stage processes (e.g., fractionation of multi-component liquid mixtures by multistage countercurrent absorber/stripping columns using supercritical CO<sub>2</sub> as solvent) requires thermodynamic models capable of predicting the chemical composition of the coexisting phases without the preliminary use of experimental data. In addition, the applied thermodynamic models must be capable to perform accurate computation of mutual solubility's of the coexisting liquid and gaseous phases in both sub-critical and critical regions [46]. However, simultaneous fulfillment of these requirements is a very difficult and challenging task for EOS [47,48].

Wheat straw was received in chopping lengths of 4–5 cm from the inaccuracy of EOS to predict the chemical composition and the mutual solubility's of the coexisting phases in both the sub-critical and critical regions for complex systems/CO<sub>2</sub>, may be overcome if phase equilibrium data for some of the binary pairs (multi-component mixture compounds)<sub>-i</sub>/CO<sub>2</sub> are available in the literature [46].

A key point in this approach is to determine the binary interaction parameters binary  $k_{aij}$  and  $k_{bij}$  by correlating phase equilibrium data for the binary pairs (multi-component mixture compounds)<sub>-i</sub>/CO<sub>2</sub> available in the literature [46]. Knowledge of binary interaction parameters makes it possible to construct the matrix of binary interaction parameters [46].

The RK-Aspen EOS with the van der Waals mixing rules and RK-Aspen combining rules for two temperature-independent binary interaction parameters  $k_{aij} = k_{aij}^0$  and

$k_{bij} = k_{bij}^0$ , and the  $k_{ij}$  between two components  $i$  and  $j$  is a function of the pure component critical properties ( $T_{ci}$ ,  $T_{cj}$ ,  $P_{ci}$ ,  $P_{cj}$ ) and acentric factors ( $\omega_i$ ,  $\omega_j$ ). In this sense, it is necessary to compute the critical properties and acentric factors of all the chemical species present in the composition of complex/multi-component mixture [46].

EOS of van der Waals type with van der Waals quadratic mixing rules, including the PR-EOS with van der Waals quadratic mixing rules, PR-EOS with quadratic mixing rules, PR-EOS with a temperature dependent binary interaction parameter  $k_{ij}$ , computed by a group contribution method, applied to predict high-pressure phase equilibrium for the binary systems carboxylic acids-CO<sub>2</sub>, hydrocarbons-CO<sub>2</sub>, and fat-soluble substances-CO<sub>2</sub> [45–55]. Most studies analyzed the thermodynamic modeling of binary systems carboxylic acids-CO<sub>2</sub>, alkanes-CO<sub>2</sub>, alkenes-CO<sub>2</sub>, cycloalkanes-CO<sub>2</sub>, cycloalkenes-CO<sub>2</sub>, aromatics-CO<sub>2</sub>, alcohols-CO<sub>2</sub>, fat-soluble substances-CO<sub>2</sub>, and fatty alcohols-CO<sub>2</sub> [45–55], representing the majority of the binary pairs OLP- $i$ /CO<sub>2</sub>, but also complex multi-component systems/CO<sub>2</sub> [45,46]. In addition, group contribution (GC) method combined with the perturbed-chain SAFT (PC-SAFT) and variable-range SAFT (VR-SAFT) EOS, applied to predict high-pressure phase equilibrium for the binary systems  $n$ -alkanes/CO<sub>2</sub> [56].

Modeling of high-pressure phase equilibrium includes the application of PR-EOS with van der Waals quadratic mixing rules for the binary systems pentane-CO<sub>2</sub> and toluene-CO<sub>2</sub> [49], PR-EOS with van der Waals quadratic mixing rules for the binary systems palmitic acid-CO<sub>2</sub>, oleic acid-CO<sub>2</sub>, linoleic acid-CO<sub>2</sub>, stigmasterol-CO<sub>2</sub>,  $\alpha$ -tocopherol-CO<sub>2</sub>, squalene-CO<sub>2</sub>, and the complex multi-component system Soy Oil Deodorizer Distillates (SODD)-SC-CO<sub>2</sub>, lumped as a mixture of key compounds palmitic acid, oleic acid, linoleic acid, stigmasterol,  $\alpha$ -tocopherol, and squalene [45], PR-EOS with quadratic mixing rules for the binary systems toluene-CO<sub>2</sub>, benzene-CO<sub>2</sub>, and  $n$ -hexane-CO<sub>2</sub> [50], PR-EOS with a group contribution method to estimate the binary interaction parameters  $k_{ij}$  for 54 (fifty four) binary systems hydrocarbons-CO<sub>2</sub> [47], PPR78 EOS with temperature dependent  $k_{ij}$  calculated using group contribution method to systems containing aromatic compounds-CO<sub>2</sub> [48], cubic EOS (PR, 3P1T, and PR-DVT), and EOS with association term (PR-CPA EOS, AEOS, SAFT, and SAFT-CB) for the binary systems  $o$ -cresol-CO<sub>2</sub>,  $p$ -cresol-CO<sub>2</sub>, and ternary system  $o$ -cresol- $p$ -cresol-CO<sub>2</sub> [51], SRK EOS with association model to correlate the solubility's of fatty acids (myristic acid, palmitic acid and stearic acid) and fatty alcohols (1-hexadecanol, 1-octadecanol, and 1-icosanol in SC-CO<sub>2</sub> [52], RK-Aspen and PR-BM EOS for the binary systems oleic acid-CO<sub>2</sub>, triolein-CO<sub>2</sub>, using the ASPEN-plus<sup>®</sup> software to predict high-pressure phase equilibrium of multicomponent mixture vegetable oil-CO<sub>2</sub>, lumped as a mixture of key compounds oleic acid and triolein, thus represented by the ternary system oleic acid-triolein-CO<sub>2</sub> [53], RK-Aspen, PR-BM and SR-POLAR EOS for the binary systems  $n$ -dodecane-CO<sub>2</sub>, 1-decanol-CO<sub>2</sub>, and 3,7-dimethyl-1-octanol-CO<sub>2</sub>, for the ternary system  $n$ -dodecane-1-decanol-CO<sub>2</sub>,  $n$ -dodecane-3,7-dimethyl-1-octanol-CO<sub>2</sub>, 3,7-dimethyl-1-octanol-1-decanol-CO<sub>2</sub>, and the quaternary system  $n$ -dodecane-3,7-dimethyl-1-octanol-1-decanol-CO<sub>2</sub>, using the ASPEN-plus<sup>®</sup> software to predict high-pressure phase equilibrium of multi-component mixture  $n$ -dodecane-3,7-dimethyl-1-octanol-1-decanol-CO<sub>2</sub> [54], PPC-SAFT EOS to predict the global behavior of the binary pair  $n$ -alkanes-CO<sub>2</sub> [55], GC-SAFT EOS (Perturbed-Chain SAFT and Variable-Range SAFT) for the binary systems  $n$ -alkanes-CO<sub>2</sub>, including propane-CO<sub>2</sub>,  $n$ -butane-CO<sub>2</sub>,  $n$ -pentane-CO<sub>2</sub>,  $n$ -hexane-CO<sub>2</sub>,  $n$ -heptane-CO<sub>2</sub>,  $n$ -octane-CO<sub>2</sub>,  $n$ -decane-CO<sub>2</sub>,  $n$ -dodecane-CO<sub>2</sub>,  $n$ -tetradecane-CO<sub>2</sub>,  $n$ -eicosane-CO<sub>2</sub>,  $n$ -docosane/CO<sub>2</sub>,  $n$ -octacosane/CO<sub>2</sub>,  $n$ -dotriacontane/CO<sub>2</sub>,  $n$ -hexatriacontane/CO<sub>2</sub>, and  $n$ -tetratriacontane-CO<sub>2</sub> [56], RK-Aspen for the binary systems organic liquid products compounds- $i$ -CO<sub>2</sub>, including undecane-CO<sub>2</sub>, tetradecane-CO<sub>2</sub>, pentadecane-CO<sub>2</sub>, hexadecane-CO<sub>2</sub>, octadecane-CO<sub>2</sub>, palmitic acid-CO<sub>2</sub>, and oleic acid-CO<sub>2</sub>, using the Aspen-HYSYS software to predict high-pressure phase equilibrium of multi-component system PLO-SC-CO<sub>2</sub> [46].

In this work, the thermodynamic data basis and EOS modeling necessary to simulate the fractionation of OLP in multistage countercurrent absorber/stripping columns using SC-CO<sub>2</sub> as solvent, with Aspen-HYSYS was systematically constructed. The physical ( $\rho$ ),

critical properties ( $T_b$ ,  $T_c$ ,  $P_c$ ,  $V_c$ ), and acentric factor ( $\omega$ ) of all the compounds present in OLP predicted by the group contribution methods of Marrero-Gani, Han-Peng, Marrero-Pardillo, Constantinou-Gani, Joback and Reid, and Vetere. The RK-Aspen applied to correlate the experimental phase equilibrium data of binary systems organic liquid products compounds (OLP)- $\text{CO}_2$  available in the literature. The regressions show that RK-Aspen EOS was able to describe the experimental phase equilibrium data for all the binary pairs (multi-component mixture compounds)- $\text{CO}_2$  under investigation.

## 2. Modeling and Simulation Methodology

### 2.1. Thermodynamic Modeling

#### 2.1.1. Prediction of Thermo-Physical ( $T_b$ ), Critical Properties ( $T_c$ , $P_c$ , $V_c$ ), and Acentric Factor ( $\omega$ ) of OLP Compounds

Predictive methods selected by considering their applicability to describe the chemical structure of molecules, including the effects of carboxylic acids and hydrocarbons chain length and molecular weight, and simplicity of use.

Experimental data of normal boiling temperature ( $T_b$ ) and critical properties ( $T_c$ ,  $P_c$ ,  $V_c$ ) of carboxylic acids [57,58], esters of carboxylic acids [57,58], hydrocarbons [59,60], and alcohols [58–61], reported by Ambrose and Ghiasse [57], Simmrock et al. [58], Danner and Daubert [59], Yaws [60], and Teja et al. [61], as well as vapor pressure ( $P^{\text{Sat}}$ ) data reported by Ambrose and Ghiasse [57], and Boublik et al. [62], used to evaluate all the methods applied to predict the thermo-physical ( $T_b$ ), critical properties ( $T_c$ ,  $P_c$ ,  $V_c$ ), and acentric factor ( $\omega$ ) of OLP compounds described in Table S1 (Supplementary Material).

Based on the chemical composition of OLP described in Table S1, experimental data for critical properties available in the literature selected to the following class of hydrocarbons including alkanes from  $\text{C}_2$ - $\text{C}_{20}$ , cyclic from  $\text{C}_3$ - $\text{C}_{17}$ , alkenes with only one double bond from  $\text{C}_4$ - $\text{C}_{20}$ , and aromatics from  $\text{C}_6$ - $\text{C}_{15}$ , carboxylic acids of linear chain length from  $\text{C}_1$ - $\text{C}_{10}$ , as well as  $\text{C}_{16}$ ,  $\text{C}_{18}$ ,  $\text{C}_{20}$ , and  $\text{C}_{22}$ , carboxylic acids with one or two double bonds including  $\text{C}_{16:1}$ ,  $\text{C}_{16:2}$ ,  $\text{C}_{18:1}$ ,  $\text{C}_{18:2}$ ,  $\text{C}_{20:1}$ ,  $\text{C}_{20:2}$ ,  $\text{C}_{22:1}$ ,  $\text{C}_{22:2}$ , alcohols of linear chain length from  $\text{C}_2$ - $\text{C}_{10}$ .

#### Methods to Predict Thermo-Physical ( $T_b$ ) and Critical Properties ( $T_c$ , $P_c$ , $V_c$ )

The predictive methods by Joback and Reid [63], Constantinou-Gani [64], Marrero-Marejón and Pardillo-Fontdevila [65], and Marrero-Gani [66] applied to estimate the normal boiling temperature ( $T_b$ ) and critical properties ( $T_c$ ,  $P_c$ ,  $V_c$ ) of all the compounds present in OLP. Table 1 presents the equations of all the predictive methods applied to compute  $T_b$ ,  $T_c$ ,  $P_c$ , and  $V_c$  [63–66].

**Table 1.** The equations used to predict/estimate the thermo-physical ( $T_b$ ) and critical properties ( $T_c$ ,  $P_c$ ,  $V_c$ ) of all the compounds present in OLP, by the methods of Joback and Reid [63], Constantinou and Gani [64], Marrero-Marejón and Pardillo-Fontdevila [65] and Marrero and Gani [66].

Constantinou-Gani [64]	Marrero-Gani [66]
$T_b = 204.359 \ln \left( \sum_i N_i (T_{b1i}) + W \sum_j M_j (T_{b2j}) \right)$ $T_c = 181.128 \ln \left( \sum_i N_i T_{c1i} + W \sum_j M_j T_{c2j} \right)$ $(P_c - 1.3705)^{-0.5} - 0.10022 = \sum_i N_i p_{c1i} + \sum_j M_j p_{c2j}$ $V_c + 0.00435 = \sum_i N_i v_{c1i} + \sum_j M_j v_{c2j}$	$T_b = 222.543 \ln \left( \sum_i N_i T_{b1i} + \sum_j M_j T_{b2j} + \sum_k O_k T_{b3k} \right)$ $T_c = 231.239 \ln \left( \sum_i N_i T_{c1i} + \sum_j M_j T_{c2j} + \sum_k O_k T_{c3k} \right)$ $(P_c - 5.9827)^{-0.5} - 0.108998 = \sum_i N_i P_{c1i} + \sum_j M_j P_{c2j} + \sum_k O_k P_{c3k}$ $V_c - 7.95 = \sum_i N_i V_{c1i} + \sum_j M_j V_{c2j} + \sum_k O_k V_{c3k}$
Joback & Reid [63]	Marrero-Pardillo [65]
$T_b = 198.2 + \sum n_i T_{bi}$ $T_c = T_b \left[ 0.584 + 0.965 \left( \sum n_i T_{ci} \right) - \left( \sum n_j T_{cj} \right)^2 \right]^{-1}$ $P_c = (0.113 + 0.0032 n_A - \sum n_i P_{ci})^{-2}$ $V_c = 17.5 + \sum$	$T_b = 204.66 + \sum$ $T_c = T_b / \left[ 0.5851 - 0.9286 \Sigma - \Sigma^2 \right]$ $P_c = (0.1285 - 0.0059 n_A - \Sigma)^{-2}$ $V_c = 25.1 + \Sigma$

The method by Constantinou-Gani [64], is based only on the molecular structure of molecules, being applied in two levels: the first level treats simple functional groups, also called first order groups, and the second level treats the second order groups, formed by blocks of first order groups. In the equations described in Table 1,  $T_{b1i}$ ,  $T_{c1i}$ ,  $P_{c1i}$  and  $V_{c1i}$  represent the group contribution of first order level for the corresponding properties, and  $N_i$  how many times the group  $i$  occurs in the molecule. In a similar way,  $T_{b2j}$ ,  $T_{c2j}$ ,  $P_{c2j}$  and  $V_{c2j}$  represents the group contributions of second order level, and  $M_j$  how many times the group  $j$  occurs in the molecule.

Marrero-Gani [66], proposed a method analogous to that of Constantinou-Gani [64], in which a group contribution of third order is added, whereas  $T_{b3k}$ ,  $T_{c3k}$ ,  $P_{c3k}$  and  $V_{c3k}$  represent these contributions, and  $O_k$  how many times the group  $k$  occurs in the molecule.

Joback and Reid [63], proposed a method to estimate the normal boiling temperature ( $T_b$ ) and critical properties ( $T_c$ ,  $P_c$ ,  $V_c$ ) using group contribution, where  $\Sigma$  symbolizes the sum of all the contributions of each group corresponding to the parts of a molecule. To compute the critical temperature ( $T_c$ ), Joback and Reid [63] proposed a method dependent on the normal boiling temperature ( $T_b$ ).

By the method of Joback and Reid [63],  $n_i$  is the number of contributions, while  $T_{bi}$  and  $T_{ci}$  are the normal boiling temperature and critical temperature associated to the  $i$ -th group contribution. To compute the critical pressure ( $P_c$ ), the method by Joback and Reid [63], considers the number of atoms within the molecule, where  $n_A$  specifies the number of atoms in the molecule, and  $P_{ci}$  the critical pressure associated to the  $i$ -th group contribution.

Marrero-Pardillo [65], proposed a method to predict the normal boiling temperature ( $T_b$ ) and critical properties ( $T_c$ ,  $P_c$ ,  $V_c$ ) of pure organic molecules that uses a novel structural approach. This methodology uses the interactions between the groups of charges within the molecule, instead of the simple group contribution. To estimate the critical pressure ( $P_c$ ), and likewise the method by Joback and Reid [63], this method also considers the number of atoms in the molecule.

#### Methods Selected to Predict the Acentric Factor ( $\omega$ )

The prediction of acentric factor performed by using direct group contribution methods as described by Constantinou et al. [67] and Han and Peng [68], as well as an indirect method using its definition from vapor pressure data, based on the proposal of Araújo and Meireles [69]. In this case, the correlation by Vetere [70] was used, making it possible to estimate the vapor pressure from molecular structure. Experimental values for acentric factors obtained as the follows:

- I. Predicted by using experimental data of critical properties, and experimental data of vapor pressure at  $T_r = 0.7$  [71];
- II. Predicted by using experimental values of critical properties and vapor pressure data at  $T_r = 0.7$ , computed with Wagner's equation [72], and the parameters obtained from experimental data fitting.

#### 2.1.2. Statistical Analysis of Predicted Thermo-Physical Property ( $T_b$ ), Critical Properties ( $T_c$ , $P_c$ , $V_c$ ), and Acentric Factor ( $\omega$ ) of OLP Compounds

The same criteria used by Melo et al. [73] and Araújo and Meireles [69] were used to select the best methods to predict the thermo-physical property, critical properties, and acentric factor of OLP compounds. The criteria based on statistical analysis (measurements of central tendency and dispersion).

The decisive criteria to select the best prediction methods for the thermo-physical properties, critical properties, and acentric factor are the measurement of central tendency, represented by the average relative deviation (ARD), the dispersion of deviations (R), and the standard deviation (S), using the procedures as follows:

1. The lower values for the average relative deviation (ARD) and standard deviation (S) define the best methods;

2. In cases where the lower average deviation corresponds to the higher standard deviation, or vice versa, the method is selected by the lower range of deviation (R).

The predicted data for the thermo-physical property, critical properties, and acentric factor computed by the methods and procedures described in Methods to Predict Thermo-Physical ( $T_b$ ) and Critical Properties ( $T_c$ ,  $P_c$ ,  $V_c$ ) and Methods Selected to Predict the Acentric Factor ( $\omega$ ), analyzed on basis its consistency related the physicochemical behavior expected for homologous series.

This test applied to hydrocarbons [61], by relating the thermo-physical property, critical properties, and the acentric factor with the number of carbons in carbon chain length or molecular weight of hydrocarbons.

### 2.1.3. Correlation of Phase Equilibrium Data for the Binary System OLP Compounds- $i$ -CO<sub>2</sub> EOS Modeling

The thermodynamic modeling applied to describe the OLP fractionation in a multi-stage countercurrent absorber/stripping column using SC-CO<sub>2</sub> as solvent, performed by the Redlich-Kwong Aspen EOS.

The RK-Aspen EOS equation of state applied to correlate the binary systems organic liquid products compounds- $i$ -CO<sub>2</sub> available in the literature, as described in Table 2. The RK-Aspen EOS with the van der Waals mixing rules and RK-Aspen combining rules for two temperature-independent binary interaction parameters, described in details by Table 2.

**Table 2.** The RK-Aspen EOS with the van der Waals mixing rules and RK-Aspen combining rules for two temperature-independent binary interaction parameters  $k_{aij} = k_{aij}^0$  and  $k_{bij} = k_{bij}^0$ .

		Equation of State
RK-Aspen	$P = \frac{RT}{V-b} - \frac{a(T)}{V(V+b)}$	$a = 0.42748 \frac{R^2 T_c^2}{P_c} \times \alpha(m_i, \eta_i, T_{ri}) b = 0.08664 \frac{RT_c}{P_c}$ $\alpha(m_i, \eta_i, T_{ri}) = [1 + m_i(1 - T_{ri}^{1/2}) - \eta_i(1 - T_{ri})(0.7 - T_{ri})]^2$
van der Waals (RK-Aspen)	Mixing Rules $a = \sum \sum x_i x_j a_{ij}$ $b = \sum \sum x_i x_j b_{ij}$ $a_{ij} = \left( a_{ii} a_{jj} \right)^{1/2} (1 - k_{aij})$ $b_{ij} = \frac{(b_{ii} b_{jj})}{2} (1 - k_{bij})$	$k_{aij} = k_{aij}^0 + k_{aij}^1 \frac{T}{1000}$ $k_{bij} = k_{bij}^0 + k_{bij}^1 \frac{T}{1000}$

Where  $k_{aij} = k_{aij}^0$  and  $k_{bij} = k_{bij}^0$  are the binary interaction parameters, considered as temperature-independent. The RK-Aspen binary interaction parameters obtained using the Aspen Properties computational package from Aspen Plus. The program uses the Britt-Lueck algorithm, with the Deming parameters initialization method, to perform a maximum like-hood estimation of the following objective function, described by Equation (1).

$$OF = \sum_i \left( \frac{T^e - T^c}{\sigma_T} \right)^2 + \sum_i \left( \frac{P^e - P^c}{\sigma_P} \right)^2 + \sum_i \left( \frac{x_i^e - x_i^c}{\sigma_x} \right)^2 + \sum_i \left( \frac{y_i^e - y_i^c}{\sigma_y} \right)^2 \quad (1)$$

where,  $x_i^e$  and  $y_i^e$  are the experimental compositions of  $i$ -th compound in the coexisting liquid and gaseous phases, respectively, and  $\sigma$  the standard deviations, applied to the state conditions (T, P) and  $x_i^c$  and  $y_i^c$  compositions of  $i$ -th compound predicted with EOS. The average absolute deviation (AAD) computed to evaluate the agreement between measured experimental data and the calculated/predicted results for all the binary systems investigated.

### High-Pressure Equilibrium Data for the Binary Systems OLP Compound- $i$ -CO<sub>2</sub>

Table 3 shows the experimental high-pressure gaseous-liquid equilibrium data for the binary systems OLP compound- $i$ -CO<sub>2</sub> used to compute the binary interaction parameters.

For the binary pairs OLP compounds- $\text{CO}_2$  not available in the literature,  $k_{aij} = k_{aij}^0$  and  $k_{bij} = k_{bij}^0$  were set equal to zero in the matrix of binary interaction parameters.

**Table 3.** Experimental gaseous-liquid equilibrium data for the binary pair's organic liquid products compounds- $\text{CO}_2$  used to compute the binary interaction parameters of RK-Aspen EOS [74–81].

$\text{CO}_2^+$	N	T [K]	P [bar]	References
Decane	29	319.11–372.94	34.85–160.60	Jimenez-Gallegos et al. (2006)
Undecane	18	314.98–344.46	23.73–133.88	Camacho-Camacho et al. (2007)
Tetradecane	2	344.28	155.54–162.99	Gasem et al. (1989)
Pentadecane	22	293.15–353.15	5.60–139.40	Secuianu et al. (2010)
Hexadecane	12	314.14–333.13	80.65–148.70	D'Souza et al. (1988)
Octadecane	12	534.86–605.36	10.16–61.90	Kim et al. (1985)
Palmitic acid	10	423.20–473.20	10.10–50.70	Yau et al. (1992)
Oleic acid	16	313.15–353.15	101.70–300.20	Bharath et al. (1992)

Because high-pressure phase equilibrium data for the complex system OLP- $\text{CO}_2$  is not available in the literature, the proposed methodology was tested to simulate the thermodynamic modeling by de-acidification of olive oil, represented by a quaternary model mixture oleic acid-squalene-triolein- $\text{CO}_2$ .

Table 4 summarizes the experimental high-pressure gaseous-liquid equilibrium data for the binary systems olive oil key (oleic acid, squalene, triolein) compounds- $\text{CO}_2$  used to compute the binary interaction parameters.

**Table 4.** Experimental gaseous-liquid equilibrium data for the binary systems oleic acid- $\text{CO}_2$ , squalene- $\text{CO}_2$ , and triolein- $\text{CO}_2$  used to compute the binary interaction parameters of RK-Aspen EOS [81–85].

$\text{CO}_2^+$	T [K]	P [bar]	N	References
<b>Triolein</b>	333.15, 353.15	200–500	8	Weber et al. (1999)
	313.15–333.15	153.4–310.0	8	Bharath et al. (1992)
<b>Oleic acid</b>	313–333	72.1–284.1	12	Zou et al. (1990)
	313.15–353.156	101.7–300.2	16	Bharath et al. (1992)
<b>Squalene</b>	313–333	100–350	11	Hernandez et al. (2010)
	333.15–363.15	100–350	12	Brunner et al. (2009)

#### Schematic Diagram of Phase Equilibria Data Correlation

The Aspen Properties<sup>®</sup> package program used for the regression of experimental phase equilibrium data described in Tables 3 and 4. Figure 1 illustrates the simplified schematic diagram of the main correlation steps of phase equilibria data for the binary system OLP compounds- $\text{CO}_2$ , and the binary system olive oil key (oleic acid, squalene, triolein) compounds- $\text{CO}_2$ , performed by using the Aspen Properties<sup>®</sup>.

The program provides several options showing how to perform regression, including several different types of objective functions. The default objective function is the Maximum likelihood objective function, given by Equation (1). To obtain the binary interaction parameters in Aspen Properties<sup>®</sup>, the following procedure was applied, regardless the type of system and model to which data will be correlated.

1. Choice of components;
2. Specification of the method (where the model applied for the regression of the experimental data is chosen);
3. Introduction or choice of experimental data (T-xy, P-xy, TP-x, T-x, TP-xy, T-xx, P-xx, TP-xx, TP-xy, etc.) depending on the type and information of the system; at this stage it is possible to either search for the compounds from the Aspen Properties<sup>®</sup> data base or enter experimental data manually;

- Regression of data: In this step the type of parameter, the parameters (according to the coding of the program) to be adjusted/correlated, the initial estimate and the limits for the regression chosen.

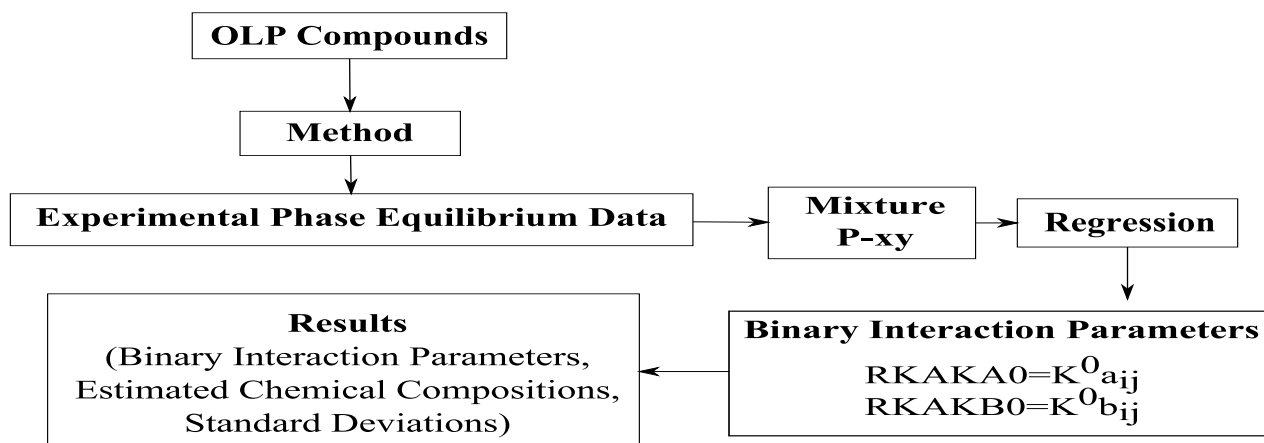


**Figure 1.** Simplified schematic diagram of the main correlation steps of phase equilibrium data for the binary system organic liquid products compounds- $i$ -CO<sub>2</sub>, and the binary system olive oil key (oleic acid, squalene, triolein) compounds- $i$ -CO<sub>2</sub>, performed by using the Aspen Properties®.

### 3. Results and Discussions

#### 3.1. Prediction of Thermo-Physical Properties and the Acentric Factor of OLP Compounds

##### 3.1.1. Normal Boiling Temperature ( $T_b$ ) of OLP Compounds

The most indicated methods, consistent with the selection criteria described in Section 2.1.2, adopted to estimate the normal boiling temperature ( $T_b$ ) of hydrocarbons classes present in OLP, illustrated in Table 5. For the  $n$ -alkanes and alkenes, the method by Marrero-Gani [66], provided the best correlation/regression to experimental data, while the method by Constantinou-Gani [64], shows the best correlation/regression for unsubstituted and substituted cyclics, and that by Joback and Reid [63], was the best for aromatics. Kontogeorgis and Tassios [86], reported that Joback and Reid [63] method was not suitable to estimate critical properties of alkanes of high molecular weight and selected Constantinou-Gani [64], as the best method.

**Table 5.** Selected methods to predict the normal boiling temperature ( $T_b$ ) of hydrocarbons classes ( $n$ -alkanes, alkenes, unsubstituted cyclics, substituted cyclics, and aromatics), of all the compounds present in OLP, obtained by thermal catalytic cracking of palm oil at 450 °C, 1.0 atmosphere, with 10% (wt.) Na<sub>2</sub>CO<sub>3</sub> [17].

Class of Hydrocarbons	N	ARD [%]	S [%]	R [%]	Methods
$n$ -Alkanes	27	−2.806	1.943	6.797	Marrero-Gani
Alkenes	19	−0.848	1.206	5.396	Marrero-Gani
Unsubstituted cyclics	9	−2.001	4.815	13.720	Constantinou-Gani
Substituted cyclics	62	−0.546	2.208	10.604	Constantinou-Gani
Aromatics	28	−0.214	1.916	7.021	Joback

##### 3.1.2. Critical Temperature ( $T_c$ ) of OLP Compounds

Table 6 shows the selected methods to predict the critical temperature ( $T_c$ ) of hydrocarbons classes ( $n$ -alkanes, alkenes, unsubstituted cyclics, substituted cyclics, and aromatics), present in OLP. The method by Marrero-Gani [66], is the most suitable for  $n$ -alkanes, alkenes, unsubstituted and unsubstituted cyclic hydrocarbons, as it showed the best correlation/regression to experimental data, while that by Constantinou-Gani [64], provided the best correlation/regression to experimental data for aromatics. Owczarek and Blazej [87] applied the methods by Joback and Reid [63] and Constantinou-Gani [64], to predict

the critical temperature ( $T_c$ ) of substituted and unsubstituted cyclic hydrocarbons, reporting deviations of 0.93% and 0.82%, respectively, when using the method by Joback and Reid [63], as well as deviations of 1.77% and 2.00%, respectively, with the method by Constantinou-Gani [64]. The results showed that computed deviations of substituted and unsubstituted cyclic hydrocarbons were 1.41% and 1.69%, respectively, when using the method by Joback and Reid [63], as well as 0.79% and 3.08%, with the method by Constantinou-Gani [64], higher than that described in Table 6, when using the method by Marrero-Gani [66]. The method by Constantinou-Gani [64] is the most suitable for aromatics. As by the estimation of normal boiling temperature ( $T_b$ ), prediction of critical temperature ( $T_c$ ) of aromatic hydrocarbons included also *n*-alkyl-benzenes, alkyl-benzenes, poly-phenyls, as well as condensed polycyclic aromatics.

**Table 6.** Selected methods to predict the critical temperature ( $T_c$ ) of hydrocarbons classes (*n*-alkanes, alkenes, unsubstituted cyclics, substituted cyclics, and aromatics), of all the compounds present in OLP, obtained by thermal catalytic cracking of palm oil at 450 °C, 1.0 atmosphere, with 10% (wt.)  $\text{Na}_2\text{CO}_3$  [17].

Class of Hydrocarbons	N	ARD [%]	S [%]	R [%]	Methods
<i>n</i> -Alkanes	15	−0.685	0.157	0.496	Marrero-Gani
Alkenes	14	0.74	0.544	2.072	Marrero-Gani
Unsubstituted cyclics	7	−0.839	2.113	5.364	Marrero-Gani
Substituted cyclics	13	0.152	1.089	3.364	Marrero-Gani
Aromatics	31	−1.192	2.233	8.415	Constantinou-Gani

### 3.1.3. Critical Pressure ( $P_c$ ) of OLP Compounds

The most indicated methods to estimate the critical pressure ( $P_c$ ) of hydrocarbons functions present in OLP are illustrated in Table 7. For *n*-alkanes, the method by Marrero-Padillo [65], provided the best results, while that by Marrero-Gani [66], selected for alkenes. For unsubstituted cyclic, the method by Joback and Reid [63], was selected. For substituted cyclic, the method by Constantinou-Gani [64], was selected. By predicting the critical pressure ( $P_c$ ) of aromatics, only the alkyl-benzenes were considered, being the method by Marrero-Gani [66], the best one. This is due to the high average relative deviation obtained for polycyclic condensates and poly-phenyls using all the methods described in Table 1, with ADR higher than 15%, reaching for some cases (m-terphenyl-Cas 92-06-8) 45%. In this sense, none of the methods evaluated showed good precision to estimate the critical pressure ( $P_c$ ) of polycyclic condensates and poly-phenyls aromatic.

**Table 7.** Selected methods to predict the critical pressure ( $P_c$ ) of hydrocarbons classes (*n*-alkanes, alkenes, unsubstituted cyclics, substituted cyclics, and aromatics), of all the compounds present in OLP, obtained by thermal catalytic cracking of palm oil at 450 °C, 1.0 atmosphere, with 10% (wt.)  $\text{Na}_2\text{CO}_3$  [17].

Class of Hydrocarbons	N	ARD [%]	S [%]	R [%]	Methods
<i>n</i> -alkanes	17	3.749	2.12	6.996	Marrero-Pardillo
alkenes	16	0.353	2.781	10.809	Marrero-Gani
Unsubstituted cyclics	7	−0.47	2.355	6.593	Joback
Substituted cyclics	14	1.537	2.939	12.782	Constantinou-Gani
Aromatics	18	0.461	2.035	9.486	Marrero-Gani

### 3.1.4. Critical Volume ( $V_c$ ) of OLP Compounds

Table 8 shows the selected methods to predict the critical volume ( $V_c$ ) of hydrocarbons classes (*n*-alkanes, alkenes, unsubstituted cyclics, substituted cyclics, and aromatics), present in OLP. The method by Marrero-Gani [66], is the most suitable for *n*-alkanes and substituted cyclic hydrocarbons, as it showed the best correlation/regression to experimental data, while that Joback and Reid [63], selected for unsubstituted cyclic hydrocarbons. The method by Marrero-Pardillo [65], selected for alkenes, while that by

Constantinou-Gani [64], provided the best correlation/regression to experimental data for aromatics.

**Table 8.** Selected methods to predict the critical volume ( $V_c$ ) of hydrocarbons classes ( $n$ -alkanes, alkenes, unsubstituted cyclics, substituted cyclics, and aromatics), of all the compounds present in OLP, obtained by thermal catalytic cracking of palm oil at 450 °C, 1.0 atmosphere, with 10% (wt.)  $\text{Na}_2\text{CO}_3$  [17].

Class of Hydrocarbons	N	ARD [%]	S [%]	R [%]	Methods
$n$ -alkanes	8	−0.23	0.681	2.070	Marrero-Gani
alkenes	16	−0.113	1.210	4.013	Marrero-Pardillo
Unsubstituted cyclics	6	−1.024	1.359	2.215	Joback
Substituted cyclics	14	−0.318	4.832	12.717	Marrero-Gani
Aromatics	19	0.034	1.914	6.785	Constantinou-Gani

### 3.1.5. Acentric Factor ( $\omega$ ) of OLP Compounds

The selected methods to estimate the acentric factor ( $\omega$ ) of hydrocarbons classes present in OLP illustrated in Table 9. For  $n$ -alkanes and alkenes, the method by Han-Peng [68], provided the best results, while the indirect method by Vetere [70], was selected for unsubstituted cyclic, unsubstituted cyclic and aromatics.

**Table 9.** Selected methods to predict the acentric factor ( $\omega$ ) of hydrocarbons classes ( $n$ -alkanes, alkenes, unsubstituted cyclics, substituted cyclics, and aromatics), of all the compounds present in OLP, obtained by thermal catalytic cracking of palm oil at 450 °C, 1.0 atmosphere, with 10% (wt.)  $\text{Na}_2\text{CO}_3$  [17].

Class of Hydrocarbons	N	ARD [%]	S [%]	R [%]	Methods
$n$ -alkanes	16	0.033	1.943	7.703	Han-Peng
alkenes	15	0.976	5.518	20.825	Han-Peng
Unsubstituted cyclics	7	2.822	2.555	7.374	Vetere
Substituted cyclics	16	1.843	3.539	15.089	Vetere
Aromatics	14	1.323	2.105	9.39	Vetere

## 3.2. Thermodynamic Modeling of Phase Equilibrium Data for the Binary System OLP Compounds- $i$ / $\text{CO}_2$

### 3.2.1. Estimation of Thermo-Physical ( $T_b$ ), Critical Properties ( $T_c$ , $P_c$ , $V_c$ ), and Acentric factor ( $\omega$ ) of OLP Compounds

Table S2 (Supplementary Material) shows the estimated values of thermo-physical ( $T_b$ ), critical properties ( $T_c$ ,  $P_c$ ,  $V_c$ ), and acentric factor ( $\omega$ ) of OLP compounds, recommended for the main chemical compounds present in the OLP obtained by thermal-catalytic cracking of palm oil, as described by Mâncio et al. [17]. The prediction of the normal boiling temperature and critical properties of carboxylic acids and esters of carboxylic acids followed the recommendations of Araújo and Meireles [69], and for estimation of acentric factor ( $\omega$ ), the indirect method proposed by Ceriani et al. [88]. This method makes use of group contributions with high similarities to the molecular structure of carboxylic acids and esters of carboxylic acids. In addition, the method proposed by Ceriani et al. [88], also applied for estimation of critical properties of ketones, while the method of Nikitin et al. [89], applied for alcohols.

### 3.2.2. Thermo-Physical ( $T_b$ ), Critical Properties ( $T_c$ , $P_c$ , $V_c$ ), and Acentric Factor ( $\omega$ ) of Olive Oil Key (Oleic Acid, Squalene, Triolein) Compounds

The estimated values of thermo-physical ( $T_b$ ), critical properties ( $T_c$ ,  $P_c$ ,  $V_c$ ), and acentric factor ( $\omega$ ) of olive oil key (oleic acid, squalene, triolein) compounds summarized in Table 10. The values for the thermo-physical ( $T_b$ ), critical properties ( $T_c$ ,  $P_c$ ,  $V_c$ ), and acentric factor ( $\omega$ ) of olive oil model mixture compounds (oleic acid, squalene, triolein) are those predicted by the authors described in Table 4.

**Table 10.** Estimated/Predicted values of thermo-physical ( $T_b$ ), critical properties ( $T_c$ ,  $P_c$ ,  $V_c$ ), and acentric factor ( $\omega$ ) of olive oil key (oleic acid, squalene, triolein) compounds [81–85].

Compounds	Cas Number	MW	$T_b$ [°C]	$T_c$ [°C]	$P_c$ [kPa]	$V_c$ [m <sup>3</sup> /kmol]	$\omega$
Triolein	122-32-7	885.00	616.7	673.9	468.2	3.022	1.686
Oleic acid	122-80-1	282.2	353.7	579.4	1388.0	1.101	1.0787
Squalene	7683-64-9	410.7	401.2	564.9	653.0	2.052	1.398

### 3.2.3. Estimation of RK-Aspen EOS Temperature-Independent Binary Interaction Parameters for the Binary Systems Hydrocarbons-<sub>i</sub>-CO<sub>2</sub> and Carboxylic Acids-<sub>i</sub>-CO<sub>2</sub>

Table 11 presents the RK-Aspen EOS temperature-independent binary interaction parameters adjusted with experimental phase equilibrium data for the binary systems hydrocarbons-<sub>i</sub>-CO<sub>2</sub> and carboxylic acids-<sub>i</sub>-CO<sub>2</sub>, as well as the absolute mean deviation (AAD) between experimental and predicted compositions for both coexisting liquid and gaseous phases. The regressions show that RK-Aspen EOS was able to describe the high-pressure gaseous-liquid phase equilibrium data for all the systems investigated.

**Table 11.** RK-Aspen EOS temperature-independent binary interaction parameters adjusted with experimental phase equilibrium data for the binary systems hydrocarbons-<sub>i</sub>-CO<sub>2</sub> and carboxylic acids-<sub>i</sub>-CO<sub>2</sub>.

CO <sub>2</sub> <sup>+</sup>	T [K]	$k_{aij}=k_{aij}^0$	$k_{bij}=k_{bij}^0$	AADx	AADy
Undecane	314.98	0.116458	−0.008014	0.0029	0.0003
	344.46	0.103282	−0.029465	0.0030	0.0036
Tetradecane	344.28	0.099874	−0.000546	0.0003	0.0011
Pentadecane	313.15	0.093344	0.026454	0.0125	0.0020
	333.15	0.101805	0.014904	0.0067	0.0030
Hexadecane	314.14	0.083111	−0.075317	0.0117	0.0090
	333.13	0.082146	−0.081056	0.0013	0.0034
Octadecane	534.86	0.246616	0.073306	0.0010	0.0024
	605.36	0.107125	0.015525	0.0002	0.0064
Palmitic acid	423.20	−0.179556	−0.042625	0.0037	$8.93 \times 10^{-5}$
	473.20	−0.059218	−0.013329	0.0008	0.0002
Oleic acid	313.15	0.110902	0.132527	0.0039	0.0031
	333.15	0.116604	0.054485	0.0039	0.0035
	353.15	0.117892	0.049413	0.0049	0.0046

### 3.2.4. Estimation of RK-Aspen EOS Temperature-Independent Binary Interaction Parameters for the Binary Systems Olive Oil Key (Oleic Acid, Squalene, Triolein) Compounds-<sub>i</sub>-CO<sub>2</sub>

Table 12 summarizes the RK-Aspen EOS temperature independent binary interaction parameters adjusted to experimental high-pressure phase equilibria of olive oil key (oleic acid, squalene, triolein) compounds-<sub>i</sub>-CO<sub>2</sub>, used as test system to simulate the thermodynamic modeling by de-acidification of olive oil, represented by a quaternary model mixture oleic acid-squalene-triolein-CO<sub>2</sub>.

#### Equation of State (EOS) Modeling for the Binary Systems Olive Oil Key (Oleic Acid, Squalene, Triolein) Compounds-<sub>i</sub>-CO<sub>2</sub>

The thermodynamic modeling for the binary systems olive oil key (oleic acid, squalene, triolein) compounds-<sub>i</sub>-CO<sub>2</sub> performed with RK-Aspen EOS with the van der Waals mixing rules and RK-Aspen combining rules for two temperature-independent binary interaction parameters. The EOS modeling described in form P-x<sub>CO2</sub>-y<sub>CO2</sub> diagram showing a comparison between predicted and experimental high-pressure equilibrium data for the binary systems oleic acid-CO<sub>2</sub> (Bharath et al., 1992), squalene-CO<sub>2</sub> (Brunner et al., 2009),

and triolein-CO<sub>2</sub> (Weber et al., 1999), as shown in Figures 2–4, respectively. The regressions show that RK-Aspen EOS was able to describe the high pressure equilibrium data for the binary systems olive oil key (oleic acid, squalene, triolein) compounds-CO<sub>2</sub>.

**Table 12.** RK-Aspen EOS  $k_{aij} = k_{aij}^0$  and  $k_{bij} = k_{bij}^0$  adjusted with experimental phase equilibrium data for the binary systems of olive oil key compounds-CO<sub>2</sub>.

CO <sub>2</sub> <sup>+</sup>	T (K)	$k_{aij}=k_{aij}^0$	$k_{bij}=k_{bij}^0$	AADx	AADy
Triolein	313.15 <sup>(a)</sup>	0.071209	0.099779	0.0094	0.0027
	333.15 <sup>(a)</sup>	0.077653	0.096221	0.0126	0.0030
	333.15 <sup>(b)</sup>	0.078059	0.083746	0.0088	0.0003
	353.15 <sup>(b)</sup>	0.103763	0.132745	0.0050	0.0001
Squalene	333.15 <sup>(c)</sup>	0.054090	−0.023325	0.0022	0.0025
	363.15 <sup>(c)</sup>	0.047825	−0.032640	0.0031	0.0014
	313 <sup>(e)</sup>	0.065395	−0.030832	0.0151	0.0016
	333 <sup>(e)</sup>	0.067249	−0.032589	0.0128	0.0013
Oleic acid	313.15 <sup>(a)</sup>	0.115801	0.130956	0.0199	0.0031
	333.15 <sup>(a)</sup>	0.116604	0.054485	0.0084	0.0035
	353.15 <sup>(a)</sup>	0.117892	0.049413	0.0062	0.0046
	313.15 <sup>(d)</sup>	0.070093	−0.006360	0.0094	0.0051
	333.15 <sup>(d)</sup>	0.089088	0.041100	0.0002	0.0067

<sup>(a)</sup>-Bharath et al. (1992), <sup>(b)</sup>-Weber et al. (1999), <sup>(c)</sup>-Brunner et al. (2009), <sup>(d)</sup>-Zou et al. (1990), <sup>(e)</sup>-Hernandez et al. (2010).

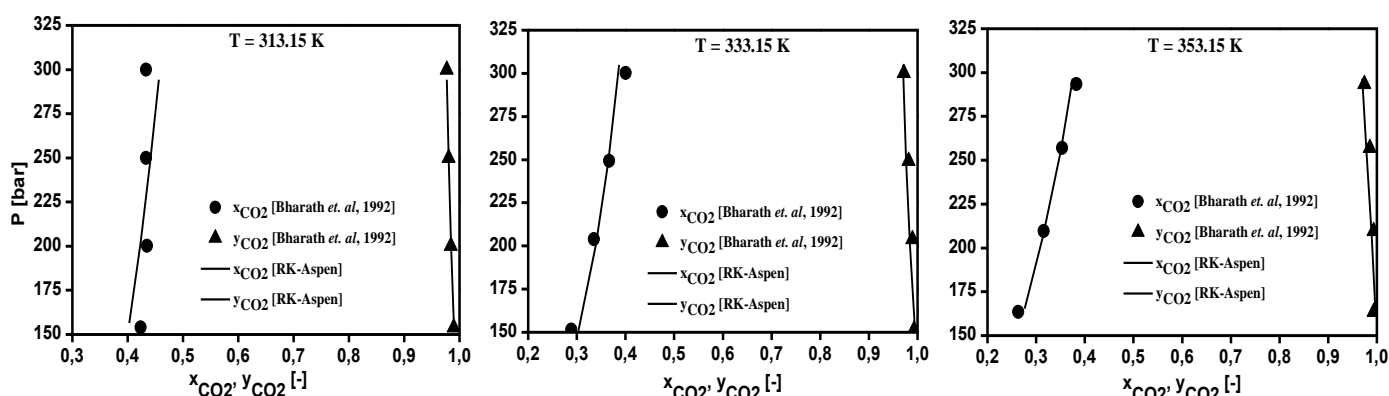


**Figure 2.** Experimental and predicted high-pressure phase equilibrium for the system oleic acid-CO<sub>2</sub> (Bharath et al., 1992).

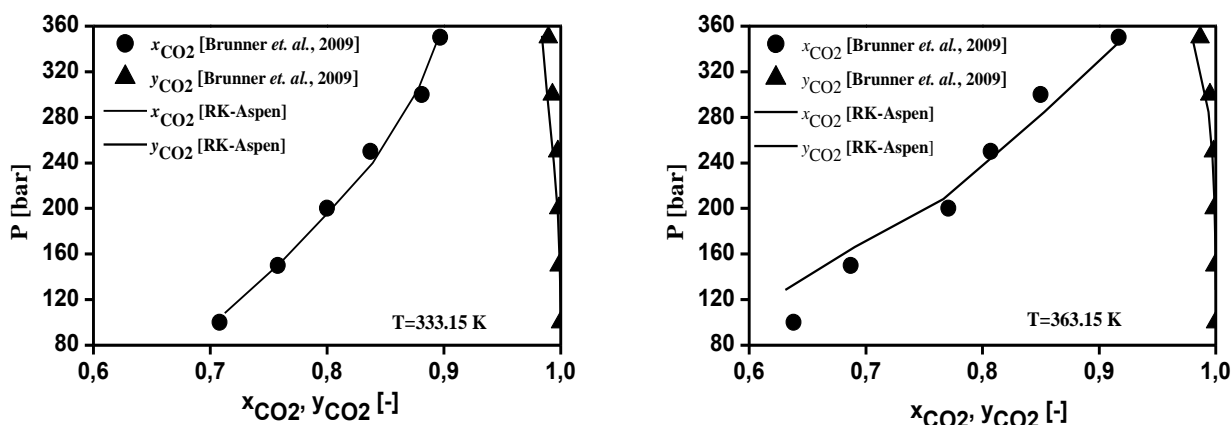


**Figure 3.** Experimental and predicted high-pressure phase equilibrium for the system squalene-CO<sub>2</sub> (Brunner et al., 2009).

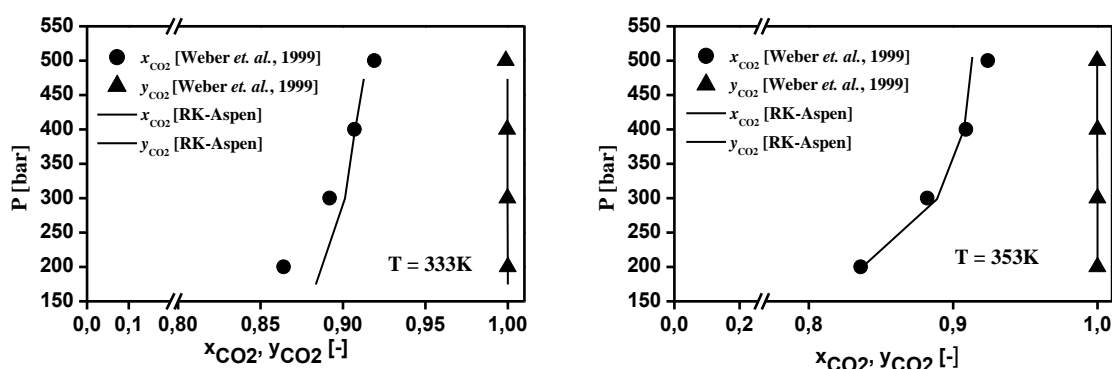


Figure 4. Experimental and predicted high-pressure phase equilibrium for the system triolein-CO<sub>2</sub> (Weber et al., 1999).

#### Simulation Modeling for the Model System Olive Oil Key (Oleic Acid-Squalene-Triolein-CO<sub>2</sub>)

Because high-pressure phase equilibrium data for the complex system OLP-CO<sub>2</sub> is not available in the literature, the proposed methodology tested to simulate the thermodynamic modeling by de-acidification of olive oil, represented by a quaternary model mixture oleic acid-squalene-triolein-CO<sub>2</sub>.

Table 13 presents the RK-Aspen EOS temperature independent binary interaction parameters adjusted to the experimental high-pressure equilibrium data for the multicomponent olive oil-CO<sub>2</sub>, described in Table 14 [90], and represented in this work as a multicomponent model mixture oleic acid-squalene-triolein-CO<sub>2</sub>. In addition, Table 13 presents the root-mean-square deviation (RMSD) between the multicomponent experimental high-pressure equilibrium data and the computed results for the coexisting gaseous-liquid phases.

The State conditions (T, P) by the experimental high-pressure equilibrium data for the multicomponent olive oil-CO<sub>2</sub>, described in Table 14.

Table 15 presents the average absolute deviation (AAD) between the predicted and experimental high-pressure phase equilibrium data for the model systems oleic acid(1)-squalene(3)-triolein(2)-CO<sub>2</sub>(4).

Table 13. RK-Aspen EOS temperature-independent binary interaction parameters adjusted with experimental high-pressure phase equilibrium data for the model systems oleic acid(1)-squalene(3)-triolein(2)-CO<sub>2</sub>(4).

$k_{ij}$	1–2	1–3	1–4	2–3	2–4	3–4	RMSD <sub>x</sub>	RMSD <sub>y</sub>
FFA in feed = 2.9 [wt.%], T[K] = 313								
$k_{aij}^0$	−1.44168	1.00000	−1.56772	−0.47399	0.08331	−0.54788	0.0014	$2.0 \times 10^{-6}$
$k_{bij}^0$	0.94017	−0.12023	−2.27950	1.00000	0.26809	−0.52108		
FFA in feed = 2.9 [wt.%], T[K] = 323								
$k_{aij}^0$	−1.78375	1.00000	−2.19466	−1.26916	0.06593	−0.90195	0.0017	$2.8 \times 10^{-5}$
$k_{bij}^0$	1.97388	0.32731	−3.32627	−0.36925	0.31781	−0.87789		
FFA in feed = 5.2 [wt.%], T[K] = 338								
$k_{aij}^0$	2.44416	−0.68874	2.65877	−0.07842	0.00445	0.40698	3.0E-07	$2.0 \times 10^{-8}$
$k_{bij}^0$	2.16063	0.99919	1.77156	0.08648	0.37099	−1.22870		
FFA in feed = 5.2 [wt.%], T[K] = 353								
$k_{aij}^0$	0.05504	0.13002	0.14571	0.16947	0.08930	0.43896	0.0058	$7.4 \times 10^{-7}$
$k_{bij}^0$	0.12297	−0.66975	0.00107	−0.91096	0.18358	0.66131		
FFA in feed = 7.6 [wt.%], T[K] = 313								
$k_{aij}^0$	−0.39597	0.95245	−0.41348	−0.40686	0.06993	−0.16959	0.0010	0.0002
$k_{bij}^0$	0.74176	−4.75749	−0.76430	0.70767	0.27402	0.22365		
FFA in feed = 15.3[wt.%], T[K] = 338								
$k_{aij}^0$	1.89568	0.99648	2.17462	0.31810	0.06235	−0.22787	0.0007	$6.9 \times 10^{-5}$
$k_{bij}^0$	0.75657	0.51874	2.50669	0.92458	0.20835	0.54779		

**Table 14.** State conditions (T, P) by high-pressure phase equilibrium data for the system olive oil-CO<sub>2</sub> [90].

FFA [wt.%]	T [K]	P [bar]	N	Reference
2.9	313	138–275	4	Simões and Brunner (1996)
	323	182–257	3	
5.2	338	190–280	2	
	353	210–298	3	
7.6	313	180–281	3	
	323	179–212	2	
15.3	313	180–302	3	
	338	21–259	2	
	353	212–303	3	

**Table 15.** The average absolute deviation (AAD) between the predicted and experimental high-pressure phase equilibrium data for the model systems oleic acid(1)-squalene(3)-triolein(2)-CO<sub>2</sub>(4).

AAD									
FFA in Feed [wt.%]	T [K]	x <sub>1</sub>	x <sub>2</sub>	x <sub>3</sub>	x <sub>4</sub>	y <sub>1</sub>	y <sub>2</sub>	y <sub>3</sub>	y <sub>4</sub>
2.9	313	0.0062	0.1906	0.0017	0.1828	0.0000	0.0002	0.0000	0.0003
2.9	323	0.0164	0.2310	0.0028	0.2118	0.0020	0.0027	0.0006	0.0027
5.2	338	0.0000	0.0000	0.0000	0.0000	0.0000	0.0000	0.0000	0.0000
5.2	353	0.0215	0.7240	0.0033	0.7082	0.0001	0.0001	0.0000	0.0001
7.6	313	0.0164	0.1274	0.0014	0.1097	0.0093	0.0225	0.0009	0.0324
15.3	338	0.0090	0.0908	0.0003	0.0816	0.0053	0.0059	0.0000	0.0112

Table 16 presents the RK-Aspen EOS temperature independent binary interaction parameters adjusted in this work to experimental high-pressure equilibrium for the system olive oil-CO<sub>2</sub> at 313 K with 2.9 and 7.6 [wt.%] FFA. The RK-Aspen EOS was able to describe the high-pressure phase equilibria of multicomponent system olive oil-CO<sub>2</sub> [90], showing RMSD between 3E-07 to 0.0138 for the liquid phase and between 0.0009 to 2E-04 for the gaseous phase, by considering the system was represented by the multicomponent model mixture triolein-squalene-oleic acid-CO<sub>2</sub>.

**Table 16.** Estimated RK-Aspen-EOS binary interaction parameters for multicomponent system FFA (oleic acid)(1)-Triglyceride (triolein)(2)-Squalene(3)-CO<sub>2</sub>(4).

$k_{ij}$	1–2	1–3	1–4	2–3	2–4	3–4	RMSD <sub>x</sub>	RMSD <sub>y</sub>
FFA in feed = 2.9 and 7.6 [wt.%], T [K] = 313								
$k_{aij}^0$	−0.150477	−0.297646	−0.111520	−0.602362	0.074580	−0.802333	0.0138	0.0009
$k_{bij}^0$	0.286959	−0.614753	−0.372917	0.992085	0.127803	−0.803741		

The distribution coefficients- $K_i$  of key compounds by the experimental high-pressure phase equilibria for the multicomponent system olive oil-CO<sub>2</sub>, described on solvent free basis, as shown in Table 17. Table 17 presents the experimental distribution coefficients of FFA (1), triglyceride (2), and squalene (3) and the estimated distribution coefficients computed using the binary interaction parameter presented in Table 13. The results show the precision of RK-Aspen EOS to describe the multicomponent system for the state conditions (T, P), and free fatty acid (FFA) content in feed. The distribution coefficients described on a solvent free basis provide information about the phase in which the compounds are preferably enriched in the extract ( $K_i > 1$ ) or in the bottoms ( $K_i < 1$ ). Figures 5–7 show the distribution coefficients for the key compounds of olive oil computed on CO<sub>2</sub> free basis. The results show that FFA and squalene are preferably enriched in the extract ( $K_i > 1$ ), while the triolein is enriched in the bottoms ( $K_i < 1$ ) by de-acidification of olive oil using SC-CO<sub>2</sub> in countercurrent packed columns.

**Table 17.** The distribution coefficients- $K_i$  of key compounds FFA (1), triglyceride (2), and squalene (3), expressed on a solvent free basis, by the experimental high-pressure phase equilibria for the multi-component system olive oil- $\text{CO}_2$ .

FFA in Feed [wt.]/T [K]	P [bar]	$K_1 \times 10^2$		$K_2 \times 10^2$		$K_3 \times 10^2$	
		Exp	Est	Exp	Est	Exp	Est
2.9/313	138	1.09	1.08	0.09	0.09	1.71	1.71
	176	2.88	2.87	0.36	0.36	4.27	4.26
	208	4.01	4.01	0.52	0.52	4.75	4.73
	275	4.50	4.51	0.81	0.81	5.95	5.98
2.9/323	182	1.93	1.97	0.10	0.10	2.54	2.55
	206	2.68	2.83	0.25	0.25	4.03	4.30
	257	4.17	3.99	0.70	0.71	4.77	4.59
5.2/338	190	1.08	1.08	0.08	0.08	1.26	1.26
	280	4.59	4.59	0.88	0.88	5.34	5.34
5.2/353	210	2.89	2.87	0.18	0.18	2.11	2.11
	260	4.76	4.80	0.44	0.44	3.07	3.10
	298	7.11	7.08	0.88	0.86	5.13	5.17
7.6/313	180	2.32	2.48	0.28	0.28	3.45	3.67
	208	3.33	3.04	0.57	0.54	4.06	3.83
	281	4.64	4.73	0.90	0.96	5.02	4.95
15.3/338	215	2.65	2.71	0.54	0.55	7.60	7.61
	259	2.67	2.60	1.08	1.07	5.16	5.17

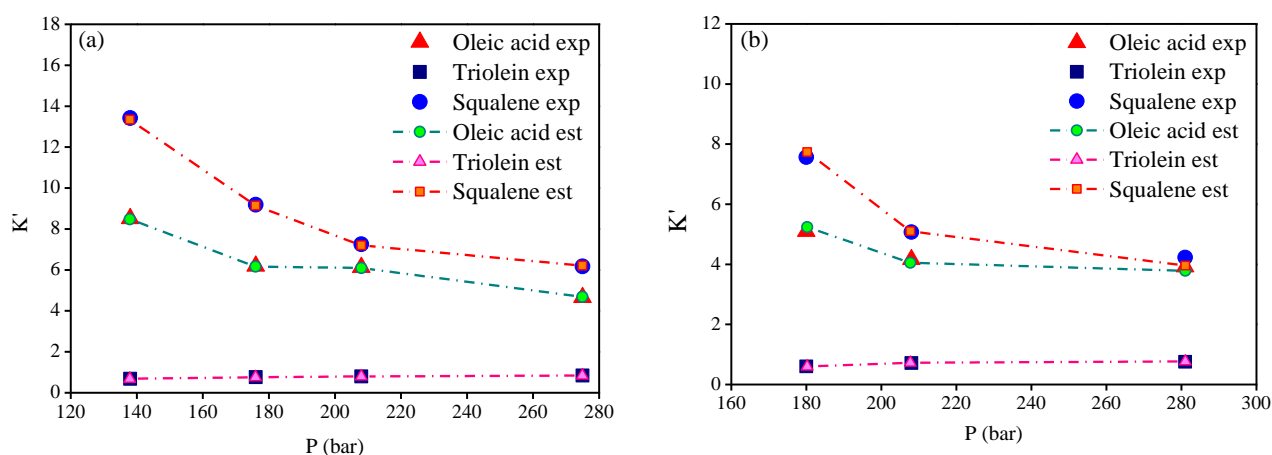


**Figure 5.** Experimental and estimated distribution coefficients  $K_i$ , expressed in  $\text{CO}_2$ -free basis, at 313 K with (a) 2.9 and (b) 7.6 [wt.%] of FFA.

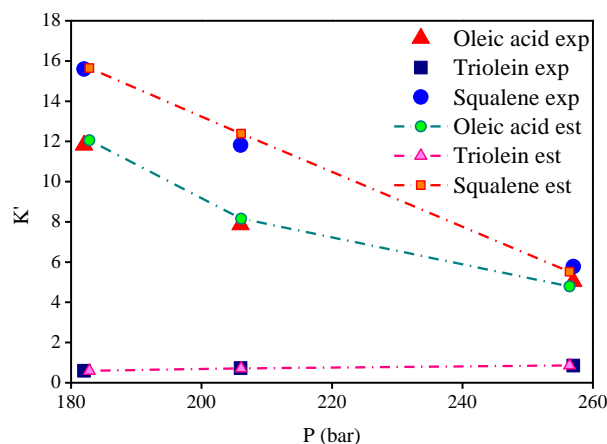


**Figure 6.** Experimental and estimated distribution coefficients  $K_i$ , expressed in  $\text{CO}_2$ -free basis, at 323 K with 2.9 [wt.%] of FFA.

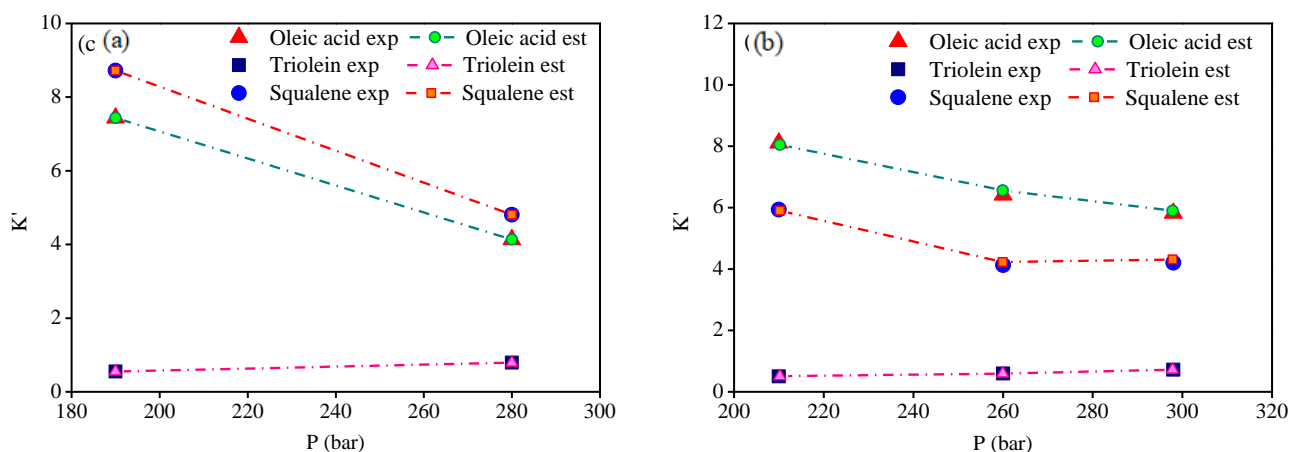


**Figure 7.** Experimental and estimated distribution coefficients  $K_i$ , expressed in  $\text{CO}_2$ -free basis, at (a) 338 and (b) 353 K with 5.2 [wt.%] of FFA.

#### 4. Conclusions

The EOS modeling described in form  $P$ - $x_{\text{CO}_2}$ ,  $y_{\text{CO}_2}$  diagram for the binary systems oleic acid- $\text{CO}_2$  (Bharath et al., 1992), squalene- $\text{CO}_2$  (Brunner et al., 2009), and triolein- $\text{CO}_2$  (Weber et al., 1999), shows that RK-Aspen EOS was able to describe the high pressure equilibrium data for the binary systems olive oil key (oleic acid, squalene, triolein) compounds- $\text{CO}_2$ .

The RK-Aspen EOS was able to describe the high-pressure phase equilibria of multicomponent system olive oil- $\text{CO}_2$  [90], showing RMSD between  $3 \times 10^{-7}$  to 0.0138 for the liquid phase and between 0.0009 to  $2 \times 10^{-4}$  for the gaseous phase, by considering the system was represented by the multicomponent model mixture triolein-squalene-oleic acid- $\text{CO}_2$ .

The proposed methodology proved to simulate with high accuracy the thermodynamic modeling by de-acidification of olive oil, represented by a quaternary model mixture oleic acid-squalene-triolein- $\text{CO}_2$ , and hence can be applied to simulate the fractionation of OLP in multistage countercurrent absorber/stripping columns using  $\text{SC-CO}_2$  as solvent, with Aspen-HYSYS.

**Supplementary Materials:** The following are available online. Table S1: Chemical composition of OLP. Table S2: Estimated/Predicted values of thermo-physical ( $T_b$ ), critical properties ( $T_c$ ,  $P_c$ ,  $V_c$ ), and acentric factor ( $\omega$ ) of chemical compounds present in OLP.

**Author Contributions:** The individual contributions of all the co-authors are provided as follows: E.C.C. contributed with formal analysis and writing—original draft preparation, W.d.A.S. contributed with EOS modeling, E.G.O.M. contributed with thermo-physical ( $T_b$ ), critical properties ( $T_c$ ,  $P_c$ ,  $V_c$ ), and acentric factor ( $\omega$ ) computations, V.M.B.C. contributed with computation of binary interaction parameters with Aspen-HYSYS, M.P.d.S. contributed with computation of binary interaction parameters with Aspen-HYSYS, M.C.S. contributed with thermal-catalytic cracking experiments, A.d.A.M. with thermal-catalytic cracking experiments, S.A.P.d.M. OLP chemical composition, M.E.A. contributed with supervision, conceptualization, and data curation, and N.T.M. contributed with supervision, conceptualization, and data curation. All authors have read and agreed to the published version of the manuscript.

**Funding:** This research was partially funded by CAPES-Brazil (2013–2016).

**Institutional Review Board Statement:** Not applicable.

**Informed Consent Statement:** Not applicable.

**Data Availability Statement:** Not applicable.

**Acknowledgments:** I would like to acknowledge Ernesto Reverchon for his marvelous contribution to supercritical fluid technology.

**Conflicts of Interest:** The authors declare no conflict of interest.

## References

1. Hua, T.; Chunyi, L.; Chaohe, Y.; Honghong, S. Alternative processing technology for converting vegetable oil and animal fats to clean fuels and light olefins. *Chin. J. Chem. Eng.* **2008**, *16*, 394–400.
2. Prado, C.M.; Filho, N.R.A. Production and characterization of the biofuels obtained by thermal cracking and thermal catalytic cracking of vegetable oils. *J. Anal. Appl. Pyrolysis* **2009**, *86*, 338–347. [[CrossRef](#)]
3. Vonghia, E.; Boocock, D.G.B.; Konar, S.K.; Leung, A. Pathways for the Deoxygenation of Triglycerides to Aliphatic Hydrocarbons over Activated Alumina. *Energy Fuels* **1995**, *9*, 1090–1096. [[CrossRef](#)]
4. Xu, J.; Jiang, J.; Sun, Y.; Chen, J. Production of hydrocarbon fuels from pyrolysis of soybean oils using a basic catalyst. *Bioresour. Technol.* **2010**, *101*, 9803–9806. [[CrossRef](#)]
5. Taufiqurrahmi, N.; Bhatia, S. Catalytic cracking of edible and non-edible oils for the production of biofuels. *Energy Environ. Sci.* **2011**, *4*, 1087–1112. [[CrossRef](#)]
6. Buzetzki, E.; Sidorová, K.; Cvengrošová, Z.; Cvengroš, J. Effects of oil type on products obtained by cracking of oils and fats. *Fuel Process. Technol.* **2011**, *92*, 2041–2047. [[CrossRef](#)]
7. Buzetzki, E.; Sidorová, K.; Cvengrošová, Z.; Kaszonyi, A.; Cvengroš, J. The influence of zeolite catalysts on the products of rapeseed oil cracking. *Fuel Process. Technol.* **2011**, *92*, 1623–1631. [[CrossRef](#)]
8. Yu, F.; Gao, L.; Wang, W.; Zhang, G.; Ji, J. Bio-fuel production from the catalytic pyrolysis of soybean oil over Me-Al-MCM-41 (Me = La, Ni or Fe) mesoporous materials. *J. Anal. Appl. Pyrolysis* **2013**, *104*, 325–329. [[CrossRef](#)]
9. Doronin, V.; Potapenko, O.; Lipin, P.; Sorokina, T. Catalytic cracking of vegetable oils and vacuum gas oil. *Fuel* **2013**, *106*, 757–765. [[CrossRef](#)]
10. Mota, S.A.P.; Mâncio, A.A.; Lhamas, D.E.L.; de Abreu, D.H.; da Silva, M.S.; dos Santos, W.G.; de Castro, D.A.R.; de Oliveira, R.M.; Araújo, M.E.; Borges, L.E.P.; et al. Production of green diesel by thermal catalytic cracking of crude palm oil (*Elaeis guineensis* Jacq) in a pilot plant. *J. Anal. Appl. Pyrolysis* **2014**, *110*, 1–11. [[CrossRef](#)]
11. Twaïq, F.A.; Mohamed, A.R.; Bhatia, S. Liquid hydrocarbon fuels from palm oil by catalytic cracking over aluminosilicate mesoporous catalysts with various Si/Al ratios. *Microporous Mesoporous Mater.* **2003**, *64*, 95–107. [[CrossRef](#)]
12. Twaïq, F.A.; Zabidi, N.A.; Bhatia, S. Catalytic Conversion of Palm Oil to Hydrocarbons: Performance of Various Zeolite Catalysts. *Ind. Eng. Chem. Res.* **1999**, *38*, 3230–3237. [[CrossRef](#)]
13. Twaïq, F.A.; Mohamad, A.R.; Bhatia, S. Performance of composite catalysts in palm oil cracking for the production of liquid fuels and chemicals. *Fuel Process. Technol.* **2004**, *85*, 1283–1300. [[CrossRef](#)]
14. Siswanto, D.Y.; Salim, G.W.; Wibisono, N.; Hindarso, H.; Sudaryanto, Y.; Ismadji, S. Gasoline Production from Palm Oil via Catalytic Cracking using MCM41: Determination of Optimum Conditions. *J. Eng. Appl. Sci.* **2008**, *3*, 42–46.
15. Sang, O.Y. Biofuel Production from Catalytic Cracking of Palm Oil. *Energy Sources* **2003**, *25*, 859–869. [[CrossRef](#)]
16. Mancio, A.D.A.; Da Costa, K.; Ferreira, C.; Santos, M.; Lhamas, D.; Mota, S.; Leão, R.; De Souza, R.; Araújo, M.; Borges, L.; et al. Process analysis of physicochemical properties and chemical composition of organic liquid products obtained by thermochemical conversion of palm oil. *J. Anal. Appl. Pyrolysis* **2017**, *123*, 284–295. [[CrossRef](#)]
17. Mancio, A.D.A.; da Costa, K.; Ferreira, C.; Santos, M.; Lhamas, D.; Mota, S.; Leão, R.; de Souza, R.; Araújo, M.; Borges, L.; et al. Thermal catalytic cracking of crude palm oil at pilot scale: Effect of the percentage of Na<sub>2</sub>CO<sub>3</sub> on the quality of biofuels. *Ind. Crop. Prod.* **2016**, *91*, 32–43. [[CrossRef](#)]
18. Dandik, L.; Aksoy, H.A.; Erdem-Senatar, A. Catalytic Conversion of Used Oil to Hydrocarbon Fuels in a Fractionating Pyrolysis Reactor. *Energy Fuels* **1998**, *12*, 1148–1152. [[CrossRef](#)]
19. Dandik, L.; Aksoy, H. Pyrolysis of used sunflower oil in the presence of sodium carbonate by using fractionating pyrolysis reactor. *Fuel Process. Technol.* **1998**, *57*, 81–92. [[CrossRef](#)]
20. Li, L.; Quan, K.; Xu, J.; Liu, F.; Liu, S.; Yu, S.; Xie, C.; Zhang, B.; Ge, X. Liquid Hydrocarbon Fuels from Catalytic Cracking of Waste Cooking Oils Using Basic Mesoporous Molecular Sieves K<sub>2</sub>O/Ba-MCM-41 as Catalysts. *ACS Sustain. Chem. Eng.* **2013**, *1*, 1412–1416. [[CrossRef](#)]
21. Ooi, Y.-S.; Zakaria, R.; Mohamed, A.R.; Bhatia, S. Catalytic Cracking of Used Palm Oil and Palm Oil Fatty Acids Mixture for the Production of Liquid Fuel: Kinetic Modeling. *Energy Fuels* **2004**, *18*, 1555–1561. [[CrossRef](#)]
22. Charusiri, W.; Vitidsant, T. Kinetic Study of Used Vegetable Oil to Liquid Fuels over Sulfated Zirconia. *Energy Fuels* **2005**, *19*, 1783–1789. [[CrossRef](#)]
23. Dandik, L.; Aksoy, H. Effect of catalyst on the pyrolysis of used oil carried out in a fractionating pyrolysis reactor. *Renew. Energy* **1999**, *16*, 1007–1010. [[CrossRef](#)]
24. Ooi, Y.S.; Zakaria, R.; Mohamed, A.R.; Bhatia, S. Synthesis of Composite Material MCM-41/Beta and Its Catalytic Performance in Waste Used palm Oil Cracking. *Appl. Catal. A Gen.* **2004**, *274*, 15–23. [[CrossRef](#)]
25. Chang, W.H.; Tye, C.T. Catalytic Cracking of Used Palm Oil Using Composite Zeolite. *Malays. J. Anal. Sci.* **2013**, *17*, 176–184.
26. Weber, B.; Stadlbauer, E.A.; Eichenauer, S.; Frank, A.; Steffens, D.; Elmar, S.; Gerhard, S. Characterization of Alkanes and Olefins from Thermo-Chemical Conversion of Animal Fat. *J. Biobased Mater. Bioenergy* **2014**, *8*, 526–537. [[CrossRef](#)]

27. Eichenauer, S.; Weber, B.; Stadlbauer, E.A. Thermochemical Processing of Animal Fat and Meat and Bone Meal to Hydrocarbons based Fuels. In Proceedings of the ASME 2015, 9th International Conference on Energy Sustainability, San Diego, CA, USA, 28 June–2 July 2015; Paper N° ES2015-49197, p. V001T02A001. [CrossRef]
28. Weber, B.; Stadlbauer, E.A.; Stengl, S.; Hossain, M.; Frank, A.; Steffens, D.; Schlich, E.; Schilling, G. Production of hydrocarbons from fatty acids and animal fat in the presence of water and sodium carbonate: Reactor performance and fuel properties. *Fuel* **2012**, *94*, 262–269. [CrossRef]
29. Wang, S.; Guo, Z.; Cai, Q.; Guo, L. Catalytic conversion of carboxylic acids in bio-oil for liquid hydrocarbons production. *Biomass Bioenergy* **2012**, *45*, 138–143. [CrossRef]
30. Bielansky, P.; Weinert, A.; Schönberger, C.; Reichhold, A. Gasoline and gaseous hydrocarbons from fatty acids via catalytic cracking. *Biomass Convers. Biorefin.* **2012**, *2*, 53–61. [CrossRef]
31. Ooi, Y.-S.; Zakaria, R.; Mohamed, A.R.; Bhatia, S. Catalytic conversion of palm oil-based fatty acid mixture to liquid fuel. *Biomass Bioenergy* **2004**, *27*, 477–484. [CrossRef]
32. Bhatia, S. Catalytic Conversion of Fatty Acids Mixture to Liquid Fuels over Mesoporous Materials. *React. Kinet. Mech. Catal. Lett.* **2005**, *84*, 295–302. [CrossRef]
33. Ooi, Y.-S.; Zakaria, R.; Mohamed, A.R.; Bhatia, S. Catalytic Conversion of Fatty Acids Mixture to Liquid Fuel and Chemicals over Composite Microporous/Mesoporous Catalysts. *Energy Fuels* **2005**, *19*, 736–743. [CrossRef]
34. Lappi, H.; Alén, R. Production of vegetable oil-based biofuels—Thermochemical behavior of fatty acid sodium salts during pyrolysis. *J. Anal. Appl. Pyrolysis* **2009**, *86*, 274–280. [CrossRef]
35. Santos, M.; Lourenço, R.; De Abreu, D.; Pereira, A.; De Castro, D.; Pereira, M.; Almeida, H.; Mancio, A.D.A.; Lhamas, D.; Mota, S.; et al. Gasoline-like hydrocarbons by catalytic cracking of soap phase residue of neutralization process of palm oil (*Elaeis guineensis* Jacq). *J. Taiwan Inst. Chem. Eng.* **2017**, *71*, 106–119. [CrossRef]
36. Almeida, H.D.S.; Correa, O.A.; Eid, J.G.; Ribeiro, H.; De Castro, D.; Pereira, M.; Pereira, L.M.; Mancio, A.D.A.; Santos, M.; Souza, J.A.; et al. Production of biofuels by thermal catalytic cracking of scum from grease traps in pilot scale. *J. Anal. Appl. Pyrolysis* **2016**, *118*, 20–33. [CrossRef]
37. Almeida, H.D.S.; Corrêa, O.; Eid, J.; Ribeiro, H.; De Castro, D.; Pereira, M.; Pereira, L.; Aâncio, A.D.A.; Santos, M.; Mota, S.; et al. Performance of thermochemical conversion of fat, oils, and grease into kerosene-like hydrocarbons in different production scales. *J. Anal. Appl. Pyrolysis* **2016**, *120*, 126–143. [CrossRef]
38. Almeida, H.D.S.; Corrêa, O.; Ferreira, C.; Ribeiro, H.; de Castro, D.; Pereira, M.; Mancio, A.D.A.; Santos, M.; Mota, S.; Souza, J.D.S.; et al. Diesel-like hydrocarbon fuels by catalytic cracking of fat, oils, and grease (FOG) from grease traps. *J. Energy Inst.* **2017**, *90*, 337–354. [CrossRef]
39. de Andrade Mancio, A. Production, Fractionation and De-Acidification of Biofuels Obtained by Thermal Catalytic Cracking of Vegetable Oils. Ph.D. Thesis, Graduate Program of Natural Resources Engineering, UFPA, Belém, Brazil, April 2015. CDD 22, Ed. 660.2995. Available online: <http://proderna.propesp.ufpa.br/ARQUIVOS/teses/Andreia.pdf> (accessed on 16 July 2021).
40. Ferreira, C.; Costa, E.; De Castro, D.; Pereira, M.; Mancio, A.D.A.; Santos, M.; Lhamas, D.; Mota, S.; Leão, A.; Duvoisin, S.; et al. Deacidification of organic liquid products by fractional distillation in laboratory and pilot scales. *J. Anal. Appl. Pyrolysis* **2017**, *127*, 468–489. [CrossRef]
41. Mancio, A.D.A.; Mota, S.; Ferreira, C.; Carvalho, T.; Neto, O.; Zamian, J.; Araújo, M.; Borges, L.; Machado, N. Separation and characterization of biofuels in the jet fuel and diesel fuel ranges by fractional distillation of organic liquid products. *Fuel* **2018**, *215*, 212–225. [CrossRef]
42. Vázquez, L.; Hurtado-Benavides, A.M.; Reglero, G.; Fornari, T.; Ibez, E.; Senorans, F.J. Deacidification of olive oil by countercurrent supercritical carbon dioxide extraction: Experimental and thermodynamic modeling. *J. Food Eng.* **2009**, *90*, 463–470. [CrossRef]
43. Zacchi, P.; Bastida, S.C.; Jaeger, P.; Cocero, M.; Eggers, R.; Alonso, M.J.C. Countercurrent de-acidification of vegetable oils using supercritical CO<sub>2</sub>: Holdup and RTD experiments. *J. Supercrit. Fluids* **2008**, *45*, 238–244. [CrossRef]
44. Machado, N.T. Fractionation of PFAD-Compounds in Countercurrent Columns Using Supercritical Carbon Dioxide as Solvent. Ph.D. Thesis, TU-Hamburg-Harburg, Hamburg, Germany, 1998.
45. Araujo, M.E.; Machado, N.T.; Meireles, M.A.A. Modeling the Phase Equilibrium of Soybean Oil Deodorizer Distillates + Supercritical Carbon Dioxide Using the Peng–Robinson EOS. *Ind. Eng. Chem. Res.* **2001**, *40*, 1239–1243. [CrossRef]
46. Costa, E.C.; Ferreira, C.C.; dos Santos, A.L.B.; da Silva Vargens, H.; Menezes, E.G.O.; Cunha, V.M.B.; da Silva, M.P.; Mancio, A.A.; Machado, N.T.; Araújo, M.E. Process simulation of organic liquid products fractionation in countercurrent multistage columns using CO<sub>2</sub> as solvent with Aspen-HYSYS. *J. Supercrit. Fluids* **2018**, *140*, 101–115. [CrossRef]
47. Vitu, S.; Privat, R.; Jaubert, J.N.; Mutelet, F. Predicting the phase equilibria of CO<sub>2</sub> + hydrocarbon systems with the PPR78 model (PR EOS and kij calculated through a group contribution method). *J. Supercrit. Fluids* **2008**, *45*, 1–26. [CrossRef]
48. Jaubert, J.N.; Vitu, S.; Mutelet, F.; Corrioum, J.P. Extension of the PPR78 model (predictive 1978, Peng–Robinson EOS with temperature dependent k<sub>ij</sub> calculated through a group contribution method) to systems containing aromatic compounds. *Fluid Phase Equilibria* **2005**, *237*, 193–211. [CrossRef]
49. Tochigi, K.; Hasegawa, K.; Asano, N.; Kojima, K. Vapor–Liquid Equilibria for the Carbon Dioxide + Pentane and Carbon Dioxide + Toluene Systems. *J. Chem. Eng. Data* **1998**, *43*, 954–956. [CrossRef]
50. Lay, E.N.; Taghikhani, V.; Ghotbi, C. Measurement and Correlation of CO<sub>2</sub> Solubility in the Systems of CO<sub>2</sub> + Toluene, CO<sub>2</sub> + Benzene, and CO<sub>2</sub> + *n*-Hexane at Near-Critical and Supercritical Conditions. *J. Chem. Eng. Data* **2006**, *51*, 2197–2200. [CrossRef]

51. Pfohl, O.; Pagel, A.; Brunner, G. Phase equilibria in systems containing o-cresol, p-cresol, carbon dioxide, and ethanol at 323.15–473.15 K and 10–35 MPa. *Fluid Phase Equilibria* **1999**, *157*, 53–79. [[CrossRef](#)]
52. Yamamoto, M.; Iwai, Y.; Nakajima, T.; Tanabe, D.; Arai, Y.; Yamamoto, M.; Iwai, Y.; Nakajima, T.; Tanabe, D.; Arai, Y. Correlation of Solubilities and Entrainer Effects for Fatty Acids and Higher Alcohols in Supercritical Carbon Dioxide Using SRK Equation of State with Association Model. *J. Chem. Eng. Jpn.* **2000**, *33*, 538–544. [[CrossRef](#)]
53. Gracia, I.; García, M.T.; Rodríguez, J.F.; Fernández, M.P.; de Lucas, A. Modelling of the phase behavior for vegetable oils at supercritical conditions. *J. Supercrit. Fluids* **2009**, *48*, 189–194. [[CrossRef](#)]
54. Zamudio, M.; Schwarz, C.E.; Knoetze, J.H. Experimental measurement and modelling with Aspen Plus® of the phase behavior of supercritical CO<sub>2</sub> + (*n*-dodecane + 1-decanol + 3,7-dimethyl-1-octanol). *J. Supercrit. Fluids* **2013**, *84*, 132–145. [[CrossRef](#)]
55. Quinteros-Lama, H.; Llovel, F. Global phase behavior in carbon dioxide plus *n*-alkanes binary mixtures. *J. Supercrit. Fluids* **2018**, *140*, 147–158. [[CrossRef](#)]
56. Le Thi, C.; Tamouza, S.; Passarello, J.-P.; Tobaly, P.; de Hemptinne, J.-C. Modeling Phase Equilibrium of H<sub>2</sub> + *n*-Alkane and CO<sub>2</sub> + *n*-Alkane Binary Mixtures Using a Group Contribution Statistical Association Fluid Theory Equation of State (GC-SAFT-EOS) with a kij Group Contribution Method. *Ind. Eng. Chem. Res.* **2006**, *45*, 6803–6810. [[CrossRef](#)]
57. Ambrose, D.; Giassee, N. Vapour pressures and critical temperatures and critical pressures of some alkanolic acids: C1 to C10. *J. Chem. Thermodyn.* **1987**, *19*, 505–519. [[CrossRef](#)]
58. Simmrock, K.H.; Janowsky, R.; Ohnsorge, A. *Critical Data of Pure Substances*; Chemistry Data Series; DECHEMA: Frankfurt, Germany, 1986; Volumes 1–2.
59. Danner, R.P.; Daubert, T.E. *Tables of Physical Thermodynamic Properties of Pure Compounds*; Design Institute for Physical Property Data (DIPPR), AIChE: New York, NY, USA, 1991.
60. Yaws, C.L. *Thermophysical Properties of Chemicals and Hydrocarbons*, 2nd ed.; William Andrew Inc.: New York, NY, USA, 2014; 809p.
61. Teja, A.; Lee, R.; Rosenthal, D.; Anselme, M. Correlation of the critical properties of alkanes and alkanols. *Fluid Phase Equilibria* **1990**, *56*, 153–169. [[CrossRef](#)]
62. Boublik, T.; Fried, V.; Hala, E. *The Vapor Pressure of Pure Substances*, 2nd ed.; Elsevier: New York, NY, USA, 1984; 980p.
63. Joback, K.; Reid, R. Estimation of pure-component properties from group-contributions. *Chem. Eng. Commun.* **1987**, *57*, 233–243. [[CrossRef](#)]
64. Constantinou, L.; Gani, R. New group contribution method for estimating properties of pure compounds. *AIChE J.* **1994**, *40*, 1697–1710. [[CrossRef](#)]
65. Marrero-Morejón, J.; Pardillo-Fontdevila, E. Estimation of pure compound properties using group-interaction contributions. *AIChE J.* **1999**, *45*, 615–621. [[CrossRef](#)]
66. Marrero, J.; Gani, R. Group-contribution based estimation of pure component properties. *Fluid Phase Equilibria* **2001**, *183–184*, 183–208. [[CrossRef](#)]
67. Constantinou, L.; Gani, R.; O’Connell, J.P. Estimation of the acentric factor and the liquid molar volume at 298 K using a new group contribution method. *Fluid Phase Equilibria* **1995**, *103*, 11–22. [[CrossRef](#)]
68. Han, B.; Peng, D.-Y. A group-contribution correlation for predicting the acentric factors of organic compounds. *Can. J. Chem. Eng.* **1993**, *71*, 332–334. [[CrossRef](#)]
69. Araújo, M.E.; Meireles, M.A. Improving phase equilibrium calculation with the Peng–Robinson EOS for fats and oils related compounds/supercritical CO<sub>2</sub> systems. *Fluid Phase Equilibria* **2000**, *169*, 49–64. [[CrossRef](#)]
70. Vetere, A. Predicting the vapor pressures of pure compounds by using the wagner equation. *Fluid Phase Equilibria* **1991**, *62*, 1–10. [[CrossRef](#)]
71. Pitzer, K.S.; Lippman, D.Z.; Curl, R.F., Jr.; Huggins, C.M.; Patersen, D.E. The volumetric and thermodynamic properties of fluids. I. Theoretical basis and virial coefficients. II. Compressibility factor, vapor pressure and entropy of vaporization. *J. Am. Chem. Soc.* **1955**, *77*, 3427–3440. [[CrossRef](#)]
72. Wagner, Z. Vapor–liquid equilibrium in the carbon dioxide-ethyl propanoate system at pressures from 2 to 9 MPa and temperatures from 303 to 323 K. *Fluid Phase Equilibria* **1995**, *112*, 125–129. [[CrossRef](#)]
73. Melo, S.A.B.V.; Mendes, M.F.; Pessoa, F.L.P. An oriented way to estimate T<sub>c</sub> and P<sub>c</sub> using the most accurate methods available. *Braz. J. Chem. Eng.* **1996**, *13*, 192–199.
74. Jiménez-Gallegos, R.; Galicia-Luna, L.A.; Elizalde-Solis, O. Experimental Vapor–Liquid Equilibria for the Carbon Dioxide + Octane and Carbon Dioxide + Decane Systems. *J. Chem. Eng. Data* **2006**, *51*, 1624–1628. [[CrossRef](#)]
75. Camacho-Camacho, L.E.; Galicia-Luna, L.A.; Elizalde-Solis, O.; Martínez-Ramírez, Z. New isothermal vapor–liquid equilibria for the CO<sub>2</sub> + *n*-nonane, and CO<sub>2</sub> + *n*-undecane systems. *Fluid Phase Equilibria* **2007**, *259*, 45–50. [[CrossRef](#)]
76. Gasem, K.A.M.; Dickson, K.B.; Dulcamara, P.B.; Nagarajan, N.; Robinson, R.L.J. Equilibrium Phase Compositions, Phase Densities, and Interfacial Tensions for CO<sub>2</sub> + Hydrocarbon Systems. CO<sub>2</sub> + *n*-Tetradecane. *J. Chem. Inf. Model* **1989**, *34*, 191–195.
77. Secuianu, C.; Ferioiu, V.; Geană, D. Phase Behavior for the Carbon Dioxide + *N*-Pentadecane Binary System. *J. Chem. Eng. Data* **2010**, *55*, 4255–4259. [[CrossRef](#)]
78. D’Souza, R.; Patrick, J.R.; Teja, A.S. High-pressure phase equilibria in the carbon dioxide-*n*-hexadecane and carbon dioxide-water systems. *Can. J. Chem. Eng.* **1988**, *66*, 319. [[CrossRef](#)]
79. Kim, H.; Lin, H.M.; Chao, K.-C. Vapor-liquid equilibrium in binary mixtures of carbon dioxide + *n*-propylcyclohexane and carbon dioxide + *n*-octadecane. *AIChE Symp. Ser.* **1985**, *84*, 96–101.

80. Yau, J.-S.; Chiang, Y.-Y.; Shy, D.-S.; Tsai, F.-N. Solubilities of carbon dioxide in carboxylic acids under high pressures. *J. Chem. Eng. Jpn.* **1992**, *25*, 544–548. [[CrossRef](#)]
81. Bharath, R.; Inomata, H.; Adschiri, T.; Arai, K. Phase equilibrium study for the separation and fractionation of fatty oil components using supercritical carbon dioxide. *Fluid Phase Equilibria* **1992**, *81*, 307–320. [[CrossRef](#)]
82. Weber, W.; Petkov, S.; Brunner, G. Vapour–liquid-equilibria and calculations using the Redlich–Kwong–Aspen-equation of state for tristearin, tripalmitin, and triolein in CO<sub>2</sub> and propane. *Fluid Phase Equilibria* **1999**, *158–160*, 695–706. [[CrossRef](#)]
83. Zou, M.; Yu, Z.; Kashulines, P.; Rizvi, S.; Zollweg, J. Fluid-Liquid phase equilibria of fatty acids and fatty acid methyl esters in supercritical carbon dioxide. *J. Supercrit. Fluids* **1990**, *3*, 23–28. [[CrossRef](#)]
84. Hernández, E.J.; Señoráns, F.J.; Reglero, G.; Fornari, T. High-Pressure Phase Equilibria of Squalene + Carbon Dioxide: New Data and Thermodynamic Modeling. *J. Chem. Eng. Data* **2010**, *55*, 3606–3611. [[CrossRef](#)]
85. Brunner, G.; Saure, C.; Buss, D. Phase Equilibrium of Hydrogen, Carbon Dioxide, Squalene, and Squalane Phase Equilibrium of Hydrogen, Carbon Dioxide, Squalene, and Squalane. *J. Chem. Eng. Data* **2009**, *54*, 1598–1609. [[CrossRef](#)]
86. Kontogeorgis, G.; Tassios, D.P. Critical constants and acentric factors for long-chain alkanes suitable for corresponding states applications. A critical review. *Chem. Eng. J.* **1997**, *66*, 35–49. [[CrossRef](#)]
87. Owczarek, I.; Blazej, K. Recommended Critical Temperatures. Part 1. Aliphatic Hydrocarbons. *ChemInform* **2004**, *35*, 541–548. [[CrossRef](#)]
88. Ceriani, R.; Gani, R.; Liu, Y.A. Prediction of Vapor Pressure and Heats of Vaporization of Edible Oil/Fat Compounds by Group Contribution. *Fluid Phase Equilibria* **2013**, *337*, 53–59. [[CrossRef](#)]
89. Nikitin, E.D.; Pavlov, P.A.; Popov, A. Critical temperatures and pressures of 1-alkanols with 13 to 22 carbon atoms. *Fluid Phase Equilibria* **1998**, *149*, 223–232. [[CrossRef](#)]
90. Simões, P.; Brunner, G. Multicomponent phase equilibria of an extra-virgin olive oil in supercritical carbon dioxide. *J. Supercrit. Fluids* **1996**, *9*, 75–81. [[CrossRef](#)]